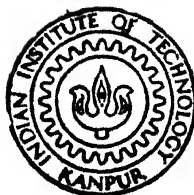# ATOMISATION OF LIQUID ALUMINIUM BY DISCRETE TYPE NITROGEN JETS

by

DEVEK NAITHANI

DEPARTMENT OF METALLURGICAL ENGINEERING

INDIAN INSTITUTE OF TECHNOLOGY KANPUR

NOVEMBER , 1991

ATOMISATION OF LIQUID ALUMINIUM BY
DISCRETE TYPE NITROGEN JETS

A Thesis submitted

in Partial Fulfilment of the Requirements

for the Degree of

MASTER OF TECHNOLOGY

by

DEVEK NAITHANI

CRoll No. 8020604)

to the

Department of Metallurgical Engineering

Indian Institute of Technology, Kanpur

November 1991

CERTIFICATE

It is certified that work contained in this thesis entitled "ATOMISATION OF LIQUID ALUMINIUM BY DISCRETE TYPE NITROGEN JETS" by Mr. Devek Naithani has been carried out under my supervision and that this work has not been submitted elsewhere for a degree.

November 1991.

Prof. R.K. Dube
Dept. of Metallurgical Engineering
I.I.T Kanpur

ME- 1994 - M-NAI-ATO

ACKNOWLEDGEMENTS

CONTENTS

ABSTRACT

The present study is concerned with the atomisation of liquid aluminium by commercial purity nitrogen jets using a discrete type confined nozzle. An attempt has been made to study the effect of process variables such as gas pressure and melt temperature on the size and size distribution of the powder.

The powder collective is defined in terms of variables such as geometric mean diameter, sauter mean diameter, volume mean diameter, and geometric standard deviation. Mathematical correlations for the yield of powder in various size ranges have been formulated. An attempt has also been made to apply the Lubanska's correlation to the present study.

CHAPTER 1

INTRODUCTION

Powder Metallurgy is an important manufacturing process by which metallic shapes are manufactured from metallic powders. The process involves production of metallic powders and its subsequent compaction and sintering to produce the final shape. Necessity of powder metallurgy arose because the conventional processes of making alloys by melting are not suitable for a number of reasons, eg. (1) difference in melting point of two elements may be so such that one would become gas before the other had melted; (2) some metals do not form a liquid solution and thus can not be alloyed; (3) melting may cause loss of identity of the constituents, eg. tungsten carbide on melting breaks down; etc.

There are many methods of manufacturing powders. The methods adopted depend to a large extent on the physical and chemical properties of the metals involved and the required size and shape of the powder particles. Mechanical pulverization is used for making powder of brittle materials such a antimony. Electrolytic process may be employed to produce powders of copper, iron, silver, and zinc etc. There are some metals such as tungsten, molybdnum, iron, and copper whose oxides can be easily reduced by a cheaper reducing agent such as hydrogen or carbon-mono-oxide, and the powder of such metal are produced by chemical reduction of their oxides. Pure metallic and alloy powders, which can be handled in molten state, can be produced by atomization. It is most popular method of producing powders for PM applications on a commercial scale and is defined as the

production of powder by the comminution of liquid metal and the subsequent freezing of the liquid droplets into powder form.

Major atomizing processes are schematically shown in Figure 1. Two fluid atomization, Figure 1(a), which accounts for approximately 95% of world's total atomizing capacity is the most common one. Here, a high velocity fluid is made to impinge on a relatively low velocity liquid metal stream which is subsequently broken up into the droplets and cooled rapidly by convection. The high velocity fluid may either be a gas or a liquid. The gases used include air, nitrogen, argon, and helium and the liquid is usually water or oil. Output in two fluid atomization can be very large, upto 20 t/hr, and the production costs are highly responsive to economies of scale.

Centrifugal atomization, Figure 1(B), is widely used for non-metals, eg. oils. In pure ultrasonic atomization, Figure 1(C), the liquid metal meets a vibrating surface and droplets are thrown off. Very low size range particles are produced with this technique. Single fluid atomization, Figure 1(D), is the process in which the molten metal is pressurized and forced through an atomizing spray jet. In electrolytic process, Figure 1(E), the liquid metal is raised to a high potential and passes to a fine nozzle where electrolytic repulsion breaks it up.

CHAPTER - 2

Gas Atomisation

2.1 Mechanism of Atomisation

In gas atomisation, a freely falling metal stream is impacted by one or more high velocity gas jets impinging the stream at an angle. The liquid stream then may take a shape of a cylindrical column, flat sheet, or a conical surface depending on the physical properties of the liquid and the surrounding gas, the velocity and pressure of the atomising gas, and the design of nozzle. Ambient atomosphere imposes rapidly growing disturbance waves on the liquid stream. At certain critical stream are torn off in the form of unstable ligaments. Ligaments, which have a very short life (less than 10^{-4} sec), breakes down into spherical drooplets due to surface tenson forces (figure-2). In atomisation using spray ring atomisers[1] with multiple gas jets, the interaction between the gas gets results in a negative pressure gradient. This causes formation of a hollow cone of the liquid sheet above the impingement point. The cone spreads laterally until the viscous and surface tension forces are unable to hold the material together as it falls under gravity and moves in the direction of increasing gas velocity. At this stage droplets are stripped from the bulk metal in a random manner. Once a cone is disintegrated, a new cone is formed and this cycle of formation and disintegration continues.

See and Johnsten[2], based on their experimental studies, identified dthree stages in gas atomisation of molten metals: primary atomistion; secondary atomisation; and solidification

(figure-3). The mechanism discussed so far discribes the primary disintegration. A drop formed in primary disintegration may be subjected to additional pressure forces and undergo further disintegration if the dynamic pressure due to gas velocity exceeds the restoring force due to surface tension The rate of solidification of droplets is important because it determines the shape of the particles. If the time for solidification is larger then the time required for surface tension forces to restore liquid droplet into a sphere and the resultant particle would be spherical in shape.

2.2 Atomising Nozzles

Two main type of nozzles used in gas atomisation of liquid metals are free fall and confined, figrue-1A In free fall, the liquid metal first fall under gravity and is atomised either by means of discrete gas jets or by an annular nozzle concentric with the metal stream. On the other hand, in confined nozzles, the liquid metal is brought to a short distance beyond the gas exit plane by means of a delivery tube and meets the gas jet in the form of a thin film. This is known to lead to more efficient breakup of the liquid, giving finer powders and is most commonly used method for production of high melting point metal powders.

2.3 Particle Size Distribution

The distribution of particle size in atomised metal powders is often found to comply with the lg-normal law. The wide range of sizes covered is its main advantage in representing satisfactorily the size distribution of gas atomised metal powders.

Size of a powder collective may be described by a mean diameter. Several such mean diameters are discussed in literature[5]. Mass median diameter, d_m, is defined as diameter of 50% point on the cummulative weight vs size graph

Sauter mean diameter, d_{vs}, is the diamter of a sphere which has the same surface area per unit volume as the powder[.] It is sensitive to changes in fine particle range of the powder collective and is expressed as :

$$d_{vs} = \frac{\Sigma \; \bar{x}^3 \; dN}{\Sigma \; \bar{x}^2 \; dN} = \frac{100}{\Sigma \; (d\phi/\bar{x})}$$

where $\bar{x}$ is mean diameter in the size band ; dN is number of particles in the band; and $d\phi$ is wt% of particles in the size band. Sauter mean diameter is emperically related[6] to process variables as:

$$d_{vs} = \frac{585}{V_{Rel}} \frac{\sqrt{\sigma}}{\sqrt{\rho}} + 597 \left[\sqrt{\frac{\mu}{\rho\sigma}} \right]^{0.45} \left[\frac{1000 \; Q_1}{Q_a} \right]^{1.5}$$

where σ is surface tension of the liquid metal; Q_1 and Q_a are mass flow rate of metal and gas respectively; and V_{Rel} is relative velocity between gas and liquid metal.

Volume mean diameter, d_{vm} a moment mean and sensitive to changes in the coarse particle range, is expressed as :

$$d_{vm} = \frac{\Sigma \; \bar{x}^4 \; dN}{\Sigma \; \bar{x}^3 \; dN} = \frac{\Sigma \; (\bar{x} \; d\phi)}{100}$$

A single mean diameter is not sufficient to describe a

powder collective as information about the spread of sizes about the mean is also necessary. This is measured by geometric standard deviation, σ_g, of the long-normal distribution and is calculated by

$$\sigma_g^5 = \frac{d_{84.1}}{d_{50}} = \frac{d_{50}}{d_{15.9}}$$

where $d_{84.1}$, d_{50} and $d_{15.9}$ are diameters of powder corresponding to cummulative weight per cent of 84.1, 50, and 15.9 respectively. A σ_g value of 1 signifies that all particles in the powder are of the same size. For σ_g values greater than 1, 84.1 wt per cent of the partifcles are smaller than the diameter of $d_m \sigma_g$. σ_g values of gas atomised aluminium powders vary from 1.8 to 2.5 depending on the mean particle size and atomising conditions.

Lubanska[7] gave a correlation in which he incorporated the effect of physical properties of the fluids. His correlation is

$$\frac{d_m}{D} = K \left[\frac{\nu_1}{\nu_g} * \frac{1}{W_e} \left(1 + \frac{m}{a} \right) \right]^{1/2}$$

where d_m is mass medium diameter; γ_1 and γ_g are kinamatic viscocities of liquid and gas respectively; m and a are mass flow rates of liquid and gas respectively; W_e is Weber number; and K is Lubanska constant. The value of K, which may reflect the influence of particle shape, is seen to vary between about 40 and 50 for a wide variety of atomising conditions.

Time for solidification of liquid metal is given by[6]

$$\tau_s = \frac{d \rho}{6 h_c} \left[C_p \ln \left(\frac{T_1 - T_g}{T_m - T_g} \right) + \frac{\Delta H_m}{T_m - T_g} \right]$$

where d is particle diameter, C_p is heat capacity of metal, T_1 is initial temperature of metal, T_g is temperature of gas, and ΔH_m is specific latent heat of fusion of metal   Convective heat transfer coefficient h_c is given by

$$h_c = \frac{k}{d} (2 + 0 \; 6 \; Re^{0 \; 5} \; Pr^{0 \; 33})$$

where K is thermal conductivity of atomising medium   Re is Reyonds's number ($\rho V d/\mu$), and Pr is Prandtal number ($\mu C_p/K$) spherodization time for droplets is given by

$$\tau_{sph} = \frac{3\pi^2 \mu}{4 V \sigma} (r_2^4 - r_1^4)$$

where r_1 is mean radius of particle, r_2 is maximum size of powder particle, and V is volume of particle of mean size

2 4 Influence of Processing Parameters

Various parameters that effect the atomisation are metal flow rate, melt temperature, nature and pressure of atomising gas, design of orifice etc   The influence of metal flow rate is important as it controls the rate of production directly   Unal[8] reported that the median diameter is often found to be proportional to the square root of the metal flow rate   This increase can be explained by the fact that with increase in the quantity of metal, the energy available per unit weight of metal decreases thus resulting in general coarseness of the product   It has been found that helium produces much finer powders than those produced by nitrogen and argon under similar conditions   This is

lower density

Keeping all other factors constant as the gas pressure is increased finer powders are produced This can be explained as gas pressure is increased greater amount of energy is available per unit weight of metal for atomisation

The melt temperature was found to have only a small effect on the powder produced This is reasonable, as the properties of metal affecting atmosisation viz density, surface tension, and viscocity depend mildly on temperature

Thompson[9], in his work discussed the influence of orifice area He found that the rate of atomisation depends linearly on the orifice area while the powder becomes coarser with increasing orifice area This also can be explained on the basis of energy available per unit weight of metal for atomisation

Subramanian[4] atomised liquid aluminium at three temperatures (1033K 1083K, and 1133K) and at line pressures below 1013 kPa He used an open type atomiser with multiple discrete nozzle jets and studied the effects of nitrogen pressure and melt temperature on the powder characteristics The powder was found to obey log-normal size distribution function with a geometric mean deviation of 2 25 being fairly independent of mean powder size and various other process variables It was found that powder size decreases as the temperature and pressure are increased At the maximum temperature and line pressure studied, i e at 1133K and 1013 kPa respectively, the geometric mean diameter was found to be 0 118 mm

Therefore there is a need to atomise liquid aluminium at line pressures above 1013 kPa so that a more complete picture of the effect of pressure and temperature on the size and size distribution of the powder may be obtained

CHAPTER - 3

AIMS OF PRESENT STUDY

(1)   To study the effect of temperature (between 933K and 1133K) and pressure (between 1013kPa and 2026kPa) on the size and size distribution of aluminium powder produced using a discrete jet type confined nozzle

(2)   To define the powder collective in terms of various size distribution functions

(3)   To determine mathematical correlations between yield and the process variables for each size fraction of powder collective

(4) To study the shape of powder produced

CHAPTER - 4

EXPERIMENTAL SET UP AND PROCEDURE

The atomisation unit schematically shown in figure-4 was setup in the first part of the project It consisted of the following components

(i)   a furnace for melting the metal
(ii)   graphite crucible with a stainless steel stopper
(iii)   an atomising nozzle
(iv)   atomisation chamber

The furnace used for melting was heated by eight silicon carbide rods Aluminium metal was kept inside the furnace in a graphite crucible A stainless steel tube of internal diameter 5 mm and length 13 cm was used to deliver the liquid metal from bottom of the crucible up to the atomising nozzle The atomising nozzle was discrete jet type having eight discrete jets converging at a point Diameter of each hole was 2 mm and angle of inclination of each hole from vertical was 35^0 The atomisation chamber was 2 m tall with square base of 1 12 m Powder was collected at the bottom of the chamber

Commercial purity aluminium was used for atomisation Standard nitrogen supplied from the cylinders was used as atomising gas

Prior to the actual runs, dry runs were performed to study the nozzle charecteristics A separate test stand was designed and nitrogen gas was passed through the nozzle Metal was not poured in dry runs The pressure at the point of impingement of gas jets was measured with the help of a pitot

tube

In the actual runs, about 500 gms of aluminium was melted in the furnace When it had attained desired temperature the gas supply was turned on and brought to the appropriate pressure and was maintained till the end of atomisation Now the liquid metal was allowed to fall from the crucible The atomised powder was collected at the bottom of the atomisation chamber and was subsequently sieve analysed BS sieves of mesh numbers 72, 100, 150 200, 300, 350, and 400 were used

Experiments were conducted at three melt temperatures – 1033K, 1083K, and 1133K while five gas pressures - 1013 kPa 1266 kPa, 1520 kPa, 1773 kPa and 2026 kPa were studied

CHAPTER - 5

RESULTS AND DISCUSSION

5 1 Relationship between Gas Pressure in the Line and Pressure at the Point of Impingement of Gas Jets

Energy required for atomising the liquid metal is obtained from the available energy at the point of impingement of gas jets This available energy is a function of pressure at that point Since it is not possible to determine the pressure at the impingeement point in actual atomisation conditions, dry runs were performed in which pressure at the point of impingement was measured The pressure at the impingement point is plotted as a function of line pressure in figure-5 Here it can be observed that the rate of increase of available energy for atomisation decreases above around 1700 kPa of line preessure ie the benificial effect of increasing line pressure goes on decreasing above 1700 kPa Unal[5] also observed above a certain pressure, no significant beneficial effect of increasing pressure He reported that pressure to be 1600 kPa However he did not specified at which point in his system he is measuring the pressure

5 2 Statistical Analysis of the Effect of Tempeerature and Pressure on Yield of the Powder

The per cent yields in various size rangees at different temperature and pressures are given in Table-1 The data was statistically analysed to determine the extent of the effect of temperature and pressure on the yield of the powder

The result of analysis of variance (ANOVA), given in Table-2, gives the values of one per cent frequence points of the F –

distribution   The calculation is shown in Appendix-1   Comparing
the theoritical and calculated F-values it is obseived that
calculated F-values for temperature are smaller than the
theoritical value with the exception of -400 mesh + Pan size
range   While the calculated F-values for pressure are higheer
than the theoritical values This shows that with in the range
investigated   temperature is not a significant   parameter
affecting yield However, some effect of temperature is observed
in the yield in -400 + Pan size fraction The gas pressure or the
line pressure has considerable effect on the yield of the powdei

Since the over all effect of temperature is negligible,
temperature-wise average of yield values at different pressures
and for different size ranges was taken for further analysis
These values are listed in Table-3 In some cases however
effect of temperature has also been considered

5 3   Mathematical Correlations for Yield of the Powder in Various
      Size Fractions

In order to mathematically formulate the effect of line pressure
on the yield of powder in various size fractions, orthogonal
polynomials were fitted on the temperature-wise mean data for
yield

Suppose yield, Y, depends on Pressure, X, as

$Y = a + bX + cX2 +$

The essential step for orthogonal fitting is to ieplace X's by
polynomials of degree i in x

ie $Y_i = A + B X_{1i} + C X_{2i} + D X_{3i} + ---$

where X_i's*   are orthogonal functions in which

$$\sum_1 X_1 = 0$$

and $$\sum_{1\ j} X_1 X_j = 0 \qquad 1 \neq j$$

Now for second order curve

$$y = A + B X_1 + C X_2$$

The error to be minimized is

$$\sum (y - A - BX_1 - CX_2)^2$$

Since it is a square, its minimum value could be zero   This leads to simultaneous equations

$$nA + B \sum X_1 + C \sum X_2 = \sum Y$$

$$A \sum X_1 + B \sum X_1^2 + C \sum X_1 X_2 = \sum X_1 Y$$

$$A \sum X_2 + B \sum X_1 X_2 + C \sum X_2^2 = \sum X_2 Y$$

Since $\sum X_1 = 0$, $\sum X_2 = 0$, and $\sum X_1 X_2 = 0$

we get

$$nA = \sum Y \quad \text{or} \quad A = \frac{\sum Y}{n}$$

$$B\sum X_1^2 = \sum X_1 Y \quad \text{or} \quad B = \frac{\sum X_1 Y}{\sum X_1^2}$$

$$C\sum X_2^2 = \sum X_2 Y \quad \text{or} \quad C = \frac{\sum X_2 Y}{\sum X_2^2}$$

So equation would be

$$Y = \frac{\Sigma Y}{n} + \left(\frac{\Sigma X_1 Y}{\Sigma X_1^2} \right) X_1 + \left(\frac{\Sigma X_2 Y}{\Sigma X_2^2} \right) X_2$$

F-values obtained by regression in the present case are compared with the standard F-values from the table[10] in order to get the order of the polynomial fitted in the data   The equations in the present study were found to be of the first degree representing a straight line   These equations are shown in Table 4

These equations are graphically represented in fig 6a-6g These figures reveal that the yield of coarse fractions of powder, i e powders of +200 mesh is decreasing with pressure while that of finer fractions is increasing   When per cent yield was plotted against impingement point pressure fig 7, nature of the plots was observed to be the same as that of between line pressure of gas and per cent yield

5 4 Powder Size Distribution

Powder collective can be represented by various size distribution functions such as normal log-normal Rosin-Rammler, etc Our results found to obey log-normal probability law Powder size was plotted against cummulative weight per cent undersize on log-normal paper   Fig 8a-8c show linear rela- tionship at all temperatures and pressures   Thus, it can be concluded that the size distribution in the present study is log-normal   This finding is consistent with that of other investigators of gas atomosation[4][5]

The equation representing log-normal distribution can be represented as[4]

$$Y = \frac{1}{\sigma_Z \sqrt{2\pi}} \exp \left\{ - \frac{(Z - \overline{Z})^2}{2 \sigma Z^2} \right\}$$

where

$$Y = \frac{d\phi}{d(\ln d)}$$

$$Z = \ln d$$

$$\overline{Z} = \frac{\Sigma Z d \phi}{\Sigma d \phi}$$

d is powder diameter

$\overline{d}$ is geometric mean diameter

ϕ is a general term for frequency, and

σ_Z is standard deviation of Z

Geometric mean diameter and geometric standard deviation which are characteristic parameters of log-normal distribution are given in table 5-6 The tables 7-9 include values for observed sauter mean diameter, volume mean diameter and Lubanska constant

5 5 Relationship between Geometric Mean Diameter and Geometric Standard Deviation

Relationship between geometric mean diameter ($\overline{d}$) and geometric standard deviation (σ_g) is depicted in fig 9   Least square calculations revealed the relationship to be

$$\sigma_g = 2 \ 115 \ (\overline{d})^{-1/43}$$

Since the slope of this curve is very small for all practical purposes σ_g can be considered to be independent of $\bar{d}$

Subramanian[4] also found σ_z to be independent of $\bar{d}$ He plotted data obtained by different investigators and found the relationship

$$\sigma_g = 2\ 25 \pm 0\ 25$$

However, σ_g varied between 2 00 and 2 14 for powders produced by him In the present study, the value of σ_g obtained is lower than that obtained by Subramanian[4] with similar nozzle design The lower σ_g value in present case may be attributed to guiding of the liquid metal stream by the delivery to be just over the point of impingement of gas sets

5 6 Effect of Pressure

5 6 1 Effect of Pressure on Sauter Mean Diameter

The effect of line pressure on sauter mean diameter is shown in fig 10 From the plots it is observed that irrespective of temperature, sauter mean diameter decreases with increasing pressure Significant decrease in sauter mean diameter is observed when temperature is increased from 1033K to 1083K Whereas there is no significant decrease when temperature is further increased upto 1133K Slope of the curves i e the rate of decrease of sauter mean diameter also decreases with increasing pressure within the range of present investigation It means that per unit reduction in d_{VS} larger pressure increase are required at

higher pressures   This can also be seen in fig 6 where   the   rate of increase of pressure   at   impingement   point   or   the   rate   of increase   of   available   energy   for   atomisation   decreases   with increasing line pressure above around 1700 kPa

5 6 2 Effect of Pressure on Geometric Mean Diameter

The influence of line pressure on geometric   mean   diameter $\bar{d}$, is shown in fig 11   It   is   observed   that $\bar{d}$ decreases   with increasing pressure   Data points are quite close at all pressures excpet only at 2026 kPa   There   is   practically   no   effect   of temperature on the Geometric mean diameter at all pressures except at 2026 kPa   (Table 5)

5 6 3 Effect of Pressure on Volume Mean Diameter

Volume mean diameter dvm,   also   showed   exactly   the   same behaviour, fig 12,   as   geometric   mean   diameter   varied   against pressure   It too decreases with pressure with some   deviation   at 2026 kPa pressure

5 7   Scanning Electron Micrographs of Aluminium Powder Produced
       by Gas Atomisation

Fig 13 shows some scanning electron micrographs of   aluminium powder   produced   in   the   present   study   Micrographs   in   fig 13(a) which are from -100 + 150 mesh range, show ligaments   having one   dimension   exceptionally   large   as   compared   to   other   two dimensions   Powder particles in fig 13(b) are of -200 + 300   mesh range   These are relatively more spherical as compared   to   those in fig 13(a)   Fig 13(c) contains micrographs of powder   particles

in -400 mesh + Pan range   Here particles   are   almost   spherical   At higher magnifications it is observed that ligaments from powder surface are   about   to   form   separate   particles   had   they   got sufficient time before solidification   Setallites   i e   small particles sticking   to   big   ones   have,   also   been   observed   in micrographs of aluminium powder

5 8   Discussion

As soon as the high velocity   gas   jets   interacts   with   the metal stream emerging out of the nozzle, primary disintegration of metal takes place   These drops are further disintegrated   into   a number of small droplets if the dynamic pressure on the drops   due to the velocity of gas is greater than the restroing force due   to surface tension   This secondary breakup occurs only if   the   drop size is   larger than a critical size corresponding to Weber   number of 13[8]   Weber number, We $= \rho \, V_{Rel}^{2} \, d/\sigma$, is the ratio   of   inertial forces to surface tension forces   This gives the   critical   value of drop size above   which   it   tend   to   disintegrate   into   small droplets

Metal temperature may effect the powder size in two   separate ways   One is through the   variation   of   liquid   properties   with temperature while the other is through   premature   solidification With increase in temperature both surface tension and viscosity of liquid metal decreases,   thus   enhancing   the   metal   breakup Therefore finer powder is expected at higher temperature   On   the other hand if the temperature   of   metal   is   too   low   premature solification may occur resulting in incomplete metal breakup

Table 10 gives the physical properties of aluminium (density surface tension and viscosity) as a function of temperature   It is observed that from 1033K to 1133K surface tension decrease by 4 per cent whereas 15 per cent decrease is observed in viscosity From the present study it is apparent that Sauter mean diameter decreases by around 20% in this temperature range (fig 11)   This decrease is mainly in the first 50° in the range   On the other hand Geometric mean diameter and volume mean diameter are insignificantly affected by temperature (fig 12 and 13)

As the pressure of gas is increased, the relative velocity between gas and liquid metal increases   Also the energy available for disintegration of unit volume of metal increases   Thus finer powder at higher pressure is obtained   The data in present study show around 25% decrase in mean diameters when pressure is increased from 1013 & kPa to 2026 & kPa

Metal head plays an important role in determining the size of powder particles   Larger metal heads result in higher velocity of metal in the stream thus getting less amount of energy per unit volume of metal for disintegration   Coarser powder is obtained in this case   On the other hand finer powder is produced in the case where metal head is low

In the present study, a fixed amount of aluminium material is used in each run keeping the initial metal head (18 Cm)   constant As the atomisation proceeds, the metal head is gradually decreased   This results in formation of a spectrum of powder sizes and having less control in determining the size distribution of the powder

The mathematical expressions given earlier for solidification time and spherodisation time are of simplified nature but they are useful for studying the effects of variables on particle shape It may be safely said that if time for solidification/time for spherodisation >> 1 than spherical shape powder is expected On the dother hand if the ratio is << 1 then irregular shape powder is expected Solidification time and spherodisation time are calculated for coarse ($\overline{d}$ = 0 150 mm) and fine ($\overline{d}$ = 0 038 mm) powder particles Calculation is given in Appendix 2 Solidification time for coarse and fine particles is found to be 8 7 msec and 6 3 msec respectively Corresponding spherodisation time are obtained for 1 43 msec and 0 36 msec respectively Thus ratio of solidification time to spherodisation time come out to be 6 and 18 respectively for coarse and fine particles In case of fine powder particle since the above ratio is >> 1, particles should be spherical in shape Perfect spherical particles are observed in fig 14-C For coarse particle the ratio is not very much greater than 1 The values near 1 will result in elongated particles approaching towards sphere as observed in fig 14-A

In the present study Lubanska constant K has been found to be in between 36 and 51 According to Lubanska[7], the constant lies in the range 40-50 In our case spherical powder is obtained in -400 mesh & Pan range (fig 14-C) while in - 100 + 150 mesh range (fig 14-A) particles are tending to become sphere)

Aluminium powder produced by Subramanian[4] has also been studied in the present investigation and the value of Lubanska constant K is found to be 65 Nozzle used by Subramanian[4] is

similar to that used in the present study He did not use delivery tube for liquid metal guidance as used in the present investigation Aspect ratio (ratio of length to bredth of a particle) of the powder produced by Subramanian[4] has been calculated by taking arithematic mean of aspect ratio of around 80 particles It came out to be 2 7 reflecting elongated particles A typical value for aspect ratio in the present study in the size range - 100 + 150 mesh is 1 2 Lubanska[7] has suggested that the constant K may reflect the influence of particle shape, but has not done any detailed study It is quite possible that the particle shape is an important factor in determining the value of K A detailed investigation is needed in this direction

CHAPTER 6

CONCLUSIONS

Following conclusions can be drawn on the basis of present investigation -

1   The rate of increase of available energy for atomisation decreases above around 1700 kPa of line pressure

2   The effect of temperature on yield in different size fractions is insignificant The effect of pressure on the yield may be mathematically represented as follows

TABLE 4   Relationship between yield in various size fractions and pressure

Size Range BSS Mesh	Equation for yield
- 72 + 100	$Y = 20\ 1 - 5\ 76\ (\frac{P-15}{5})$
- 100 + 150	$Y = 16\ 92 - 4\ 9\ (\frac{P-15}{5})$
- 150 + 200	$Y = 19\ 38 - 1\ 22\ (\frac{P-15}{5})$
- 200 + 300	$Y = 21\ 16 - 5\ 62\ (\frac{P-15}{5})$
- 300 + 350	$Y = 4\ 38 - 0\ 32\ (\frac{P-15}{5})$
- 350 + 400	$Y = 6\ 96 - 2\ 18\ (\frac{P-15}{5})$
~ 400 + PAN	$Y = 11\ 12 - 4\ 42\ (\frac{P-15}{5})$

P is pressure in Bars and Y is yield in wt %

3   Yield of coarse fractions of powder i e powder of +200 mesh decrease with increasing pressure while of finer fractions increase with pressure

4   Powder size distribution has been found to be log-normal

5   Geometric standard deviation is almost independent of geometric mean diameter in the range of present investigation   Maximum and minimum values of σ_g corresponding to $\tilde{d}_{min}$ of 0 063 mm and $\bar{d}_{max}$ of 0 105 mm are 1 92 and 1 90 respectively

6   Geometric mean diameter sauter mean diameter and volume mean diameter decrease by around 25% when pressure is increased from 1013 kPa to 2026 kPa

7   Solidification time for coarse (d = 01 50mm) and fine (d = 0 038 mm) aluminium particles is 6 and 18 times larger than the corresponding spherodisation time

8   The shape of aluminium powder in the size range -400 mesh +pan was spherical while in the size range such as -100 +150 mesh, it was elongated having aspect ratio of 1 2

9   The Lubanska constant for the atomisation process in the present study has been found to be in the range 36-51 and confirms the value suggested by Lubanska i e 40-50

CHAPTER 7

SUGGESTIONS FOR FUTURE WORK

1   Investigation should be carried out while keeping metal   head
     constant

2   Investigation should be carried out to study   the   effect   of
     particle shape   on   the   Lubanska   constant   using   the   same
     atomisation equipment

3   High speed photography   may   be   carried   out   to   study   the
     mechanics of power formation

TABLE - 1   Seive Analysis of Aluminium Powder obtained at
           different melt temperature and gass pressure

(ı)   TEMPERATURE   1033k (760°C)

                       PRESSURE   1013 kPa (10 Bars)

SIZE RANGE BSS MESH	Wt %	SIZE BSS MESH (mm)		CUMMULATIVE Wt % RETAINED
- 72 + 100	28 5	> 100	(0 15)	28 5
- 100 + 150	24 4	> 150	(0 106)	52 9
- 150 + 200	14 6	> 200	(0 075)	72 5
- 200 + 300	13 0	> 300	(0 053)	85 5
- 300 + 350	3 4	> 350	(0 045)	88 9
- 350 + 400	4 8	> 400	(0 038)	93 7
- 400 + PAN	6 4	> PAN		100

(ıı)   TEMPERATURE   1033k (760°C)

                       PRESSURE   1266 kPa (12 5 Bar)

SIZE RANGE BSS MESH	Wt %	SIZE BSS MESH (mm)		CUMMULATIVE Wt % RETAINED
- 72 + 100	24 3	> 100	(0 150)	24 3
- 100 + 150	23 8	> 150	(0 106)	48 1
- 150 + 200	10 9	> 200	(0 075)	59 0
- 200 + 300	23 9	> 300	(0 053)	82 9
- 300 + 350	5 4	> 350	(0 045)	88 3
- 350 + 400	8 6	> 400	(0 038)	96 9
- 400 + PAN	3 1	> PAN		100

(iii)   TEMPERATURE   1033k (760°C)

PRESSURE   1520 kPa (10 Bars)

SIZE RANGE BSS MESH	Wt %	SIZE BSS MESH (mm)	CUMMULATIVE Wt % RETAINED
- 72 + 100	13 3	> 100 (0 15)	13 3
- 100 + 150	18 4	> 150 (0 106)	31 1
- 150 + 200	20 4	> 200 (0 075)	52 1
- 200 + 300	26 2	> 300 (0 053)	78 3
- 300 + 350	5 7	> 350 (0 045)	84 0
- 350 + 400	8 2	> 400 (0 038)	92 2
- 400 + PAN	8 8	> PAN	100

(iv)   TEMPERATURE   1033k (760°C)

PRESSURE   1773 kPa (10 Bars)

SIZE RANGE BSS MESH	Wt %	SIZE BSS MESH (mm)	CUMMULATIVE Wt % RETAINED
- 72 + 100	16 0	> 100 (0 15)	16 0
- 100 + 150	14 7	> 150 (0 106)	30 7
- 150 + 200	21 5	> 200 (0 075)	52 2
- 200 + 300	25 9	> 300 (0 053)	78 1
- 300 + 350	4 8	> 350 (0 045)	82 9
- 350 + 400	7 3	> 400 (0 038)	90 2
- 400 + PAN	9 9	> PAN	100

(v)   TEMPERATURE   1033k (760°C)

PRESSURE   2026 kPa (20 Bar)

SIZE RANGE BSS MESH	Wt %	SIZE BSS MESH (mm)	CUMMULATIVE Wt % RETAINED
- 72 + 100	18 2	> 100 (0 15)	18 2
- 100 + 150	15 2	> 150 (0 106)	33 4
- 150 + 200	22 9	> 200 (0 075)	56 3
- 200 + 300	25 4	> 300 (0 053)	81 7
- 300 + 350	2 7	> 350 (0 045)	84 4
- 350 + 400	4 7	> 400 (0 038)	89 1
- 400 + PAN	10 9	> PAN	100

(vi)   TEMPERATURE   1083K (810°C)

PRESSURE   1013 kPa (10 Bar)

SIZE RANGE BSS MESH	Wt %	SIZE BSS MESH (mm)	CUMMULATIVE Wt % RETAINED
- 72 + 100	20 6	> 100 (0 15)	20 6
- 100 + 150	26 6	> 150 (0 106)	47 2
- 150 + 200	21 5	> 200 (0 075)	68 7
- 200 + 300	15 3	> 300 (0 053)	84 0
- 300 + 350	3 6	> 350 (0 045)	87 6
- 350 + 400	4 7	> 400 (0 038)	92 3
- 400 + PAN	7 7	> PAN	100

(vii)   TEMPERATURE   1083k (810°C)

                   PRESSURE   1266 kPa (12 5 Bar)

SIZE RANGE BSS MESH	Wt %	SIZE BSS MESH (mm)		CUMMULATIVE Wt % RETAINED
- 72 + 100	25 0	> 100	(0 15)	25 0
- 100 + 150	15 7	> 150	(0 106)	40 7
- 150 + 200	21 4	> 200	(0 075)	62 1
- 200 + 300	17 8	> 300	(0 053)	79 9
- 300 + 350	4 3	> 350	(0 045)	84 2
- 350 + 400	5 1	> 400	(0 038)	89 3
- 400 + PAN	10 6	> PAN		100

(viii)   TEMPERATURE   1083k (810°C)

                   PRESSURE   1520 kPa (15 Bar)

SIZE RANGE BSS MESH	Wt %	SIZE BSS MESH (mm)		CUMMULATIVE Wt % RETAINED
- 72 + 100	15 4	> 100	(0 15)	15 4
- 100 + 150	13 5	> 150	(0 106)	28 9
- 150 + 200	24 6	> 200	(0 075)	53 5
- 200 + 300	21 5	> 300	(0 053)	75 0
- 300 + 350	4 6	> 350	(0 045)	79 6
- 350 + 400	8 0	> 400	(0 038)	87 6
- 400 + PAN	12 5	> PAN		100

(ıx)   TEMPERATURE   1083K (810°C)

PRESSURE   1773 kPa (17 5 Baı)

SIZE RANGE BSS MESH	Wt %	SIZE BSS MESH (mm)	CUMMULATIVE Wt % RETAINED
- 72 + 100	15 6	> 100 (0 15)	15 6
- 100 + 150	14 6	> 150 (0 106)	30 2
- 150 + 200	19 0	> 200 (0 075)	49 2
- 200 + 300	25 0	> 300 (0 053)	74 2
- 300 + 350	6 1	> 350 (0 045)	80 3
- 350 + 400	7 6	> 400 (0 038)	87 9
- 400 + PAN	11 9	> PAN	100

(x)   TEMPERATURE   1083K (810°C)

PRESSURE   202b kPa (20 Bar)

SIZE RANGE BSS MESH	Wt %	SIZE BSS MESH (mm)	CUMMULATIVE Wt % RETAINED
- 72 + 100	13 9	> 100 (0 15)	13 9
- 100 + 150	10 6	> 150 (0 106)	24 5
- 150 + 200	15 3	> 200 (0 075)	39 8
- 200 + 300	28 5	> 300 (0 053)	68 3
- 300 + 350	6 1	> 350 (0 045)	74 4
- 350 + 400	10 2	> 400 (0 038)	84 6
- 400 + PAN	15 4	> PAN	100

(xi)   TEMPERATURE   1133K (860°C)

                        PRESSURE   1013 kPa (10 Bar)

SIZE RANGE BSS MESH	Wt %	SIZE BSS MESH (mm)	CUMMULATIVE Wt % RETAINED
- 72 + 100	28 0	> 100 (0 15)	28 0
- 100 + 150	20 3	> 150 (0 106)	48 3
- 150 + 200	23 2	> 200 (0 075)	71 5
- 200 + 300	13 8	> 300 (0 053)	85 3
- 300 + 350	3 3	> 350 (0 045)	88 6
- 350 + 400	4 6	> 400 (0 038)	93 2
- 400 + PAN	8 6	> PAN	100

(xii)   TEMPERATURE   1133K (860°C)

                        PRESSURE   1266 kPa (12 5 Bar)

SIZE RANGE BSS MESH	Wt %	SIZE BSS MESH (mm)	CUMMULATIVE Wt % RETAINED
- 72 + 100	26 0	> 100 (0 15)	26 0
- 100 + 150	18 3	> 150 (0 106)	44 3
- 150 + 200	21 6	> 200 (0 075)	65 9
- 200 + 300	16 6	> 300 (0 053)	82 5
- 300 + 350	3 8	> 350 (0 045)	86 3
- 350 + 400	4 5	> 400 (0 038)	90 8
- 400 + PAN	10 4	> PAN	100

(xiii)   TEMPERATURE   1133K (860°C)

PRESSURE   1520 kPa (15 Bar)

SIZE RANGE BSS MESH	Wt %	SIZE BSS MESH (mm)	CUMMULATIVE Wt % RETAINED
- 72 + 100	22 1	> 100 (0 150)	22 1
- 100 + 150	16 6	> 150 (0 106)	38 7
- 150 + 200	17 1	> 200 (0 075)	55 8
- 200 + 300	20 5	> 300 (0 053)	76 3
- 300 + 350	4 3	> 350 (0 045)	80 6
- 350 + 400	6 5	> 400 (0 038)	87 1
- 400 + PAN	12 8	> PAN	100

(xiv)   TEMPERATURE   1133K (860°C)

PRESSURE   1773 kPa (17 5 Bar)

SIZE RANGE BSS MESH	Wt %	SIZE BSS MESH (mm)	CUMMULATIVE Wt % RETAINED
- 72 + 100	20 6	> 100 (0 15)	20 6
- 100 + 150	13 1	> 150 (0 106)	33 7
- 150 + 200	16 2	> 200 (0 075)	49 9
- 200 + 300	20 7	> 300 (0 053)	70 6
- 300 + 350	5 0	> 350 (0 045)	75 6
- 350 + 400	8 0	> 400 (0 038)	83 6
- 400 + PAN	16 4	> PAN	100

(xv)

TEMPERATURE   1133K (860°C)

PRESSURE   2026 kPa (20 Bar)

SIZE RANGE BSS MESH	Wt %	SIZE BSS MESH (mm)		CUMMULATIVE Wt % RETAINED
- 72 + 100	13 8	> 100	(0 15)	13 8
- 100 + 150	10 5	> 150	(0 106)	24 3
- 150 + 200	15 4	> 200	(0 075)	39 7
- 200 + 300	23 4	> 300	(0 053)	63 1
- 300 + 350	2 5	> 350	(0 045)	65 6
- 350 + 400	12 3	> 400	(0 038)	77 9
- 400 + PAN	22 1	> PAN		100

TABLE - 2   Result of analysis of variance

Size Range BSS Mesh	Calculated Temperature	F Value Pressure
- 72 + 100	1 8	7 5
- 100 + 150	1 9	8 7
- 150 + 200	1 9	4 1
- 200 + 300	2 7	12 3
- 300 + 350	1 6	11 7
- 350 + 400	0 06	12 6
- 400 + PAN	6 0	8 1

Table [10] F-value for temp   2 1
Table [10] F-value for pressure   4 4

TABLE 3   Mean value of yield at different pressures

Size Range (BSS Mesh)	Pressure, kPa 1013	1266	1520	1773	2026
- 72 + 100	25 8	25 1	16 9	17 4	15 3
- 100 + 150	23 8	16 9	16 0	15 8	12 1
- 150 + 200	21 4	18 0	20 7	18 9	17 9
- 200 + 300	14 0	19 4	22 7	23 9	25 8
- 300 + 350	3 4	4 5	4 9	5 3	3 8
- 350 + 400	4 4	6 1	7 6	7 6	9 1
- 400 + PAN	7 4	8 0	11 4	12 7	16 1

TABLE 4   Relationship between yield in various size fractions and pressure

Size Range BSS Mesh	Equation for yield
- 72 + 100	$Y = 20\ 1 - 5\ 76\ (\frac{P-15}{5})$
- 100 + 150	$Y = 16\ 92 - 4\ 9\ (\frac{P-15}{5})$
- 150 + 200	$Y = 19\ 38 - 1\ 22\ (\frac{P-15}{5})$
- 200 + 300	$Y = 21\ 16 - 5\ 62\ (\frac{P-15}{5})$
- 300 + 350	$Y = 4\ 38 - 0\ 32\ (\frac{P-15}{5})$
- 350 + 400	$Y = 6\ 96 - 2\ 18\ (\frac{P-15}{5})$
- 400 + PAN	$Y = 11\ 12 - 4\ 42\ (\frac{P-15}{5})$

P is pressure in Bars and Y is yield in wt %

TABLE - 5   Geometric mean diameter (mm) of the powder at different temperatures and pressures

Temp K	Pressure, kPa				
	1013	1266	1520	1773	2026
1033	0 105	0 090	0 080	0 080	0 080
1083	0 096	0 085	0 076	0 076	0 068
1133	0 102	0 094	0 082	0 075	0 063

TABLE - 6   Geometric standard deviation at different
              temperatures and pressures

Temp K			Pressure, kPa		
	1013	1266	1520	1773	2026
1033	1 95	1 89	1 85	1 85	1 85
1083	1 88	1 88	1 91	1 91	1 84
1133	1 96	1 97	1 98	1 93	1 98

TABLE - 7   Sauter mean diameter (mm) at different
              temperatures and pressures

Temp K			Pressure, kPa		
	1013	1266	1520	1773	2026
1033	0 087	0 081	0 073	0 065	0 062
1083	0 072	0 065	0 058	0 057	0 051
1133	0 072	0 066	0 060	0 053	0 045

TABLE - 8   Volume mean diameter (mm) at different
              temperatures and pressures

Temp K			Pressure kPa		
	1013	1266	1520	1773	2026
1033	0 114	0 106	0 091	0 091	0 095
1083	0 106	0 102	0 089	0 089	0 081
1133	0 110	0 106	0 097	0 091	0 078

TABLE - 9   Lubanska constant at different temperatures and pressures

Temp k	Pressure, kPa				
	1013	1266	1520	1773	2026
1033	49	40	46	49	51
1083	37	42	48	36	38
1133	38	44	51	38	40

TABLE 10   Physical properties of aluminium

Density (ρ), Kg/m^3 = 2385 - 0 28 (T-933)

Surface tension (σ), N/m = {914-0 35 (T-933)} $\times$ 10^{-3}

Viscosity (μ), Ns/m^2 = {0 149 exp (16500/RT)} $\times$ 10^{-3}

Specific lateral heat of fusion[**], ΔHm = 385 18 KJ/Kg

Specific heat of liquid aluminium[**], C_ρ = 833 J/Kg-k

Values of density, surface tension and viscosity of aluminium at different temperatures used in the present study

Property	Temperature K		
	1033	1083	1133
ρ (Kg/m^3)	2357	2343	2329
σ ,N/m	0 879	0 8615	0 844
μ, Ns/m^2	1 019*10^{-3}	0 931*10^{-3}	0 859*10^{-3}

** Ref 11

TABLE - 11   Physical properties of nitrogen gas at STP

	Property	Value	Ref
1	Specific heat	1041 J/Kg-K	11
2	Thermal conductivity	0 0262 W/m-K	11
3	Density	1 142 Kg/m^3	11
4	Absolute Viscosity	17 84 * 10^{-6} Ns/m^2	11
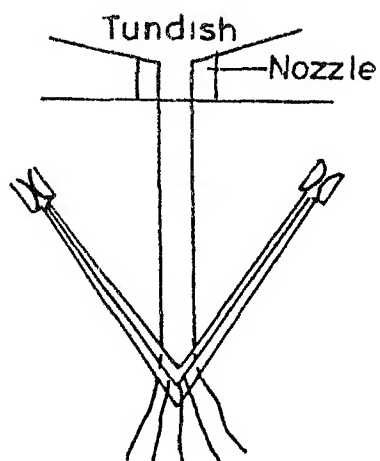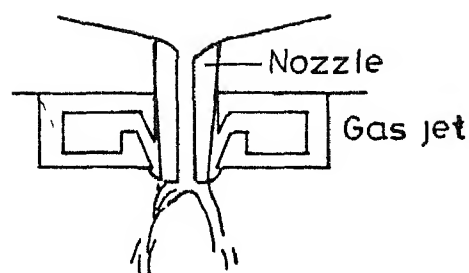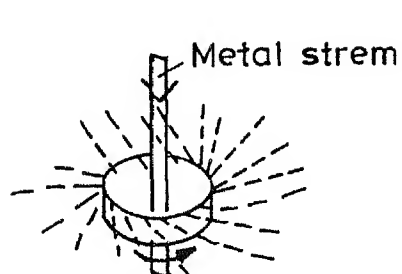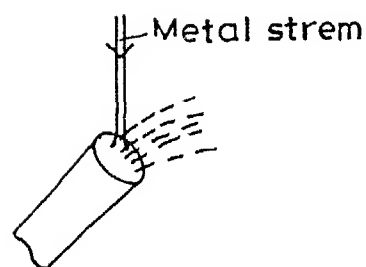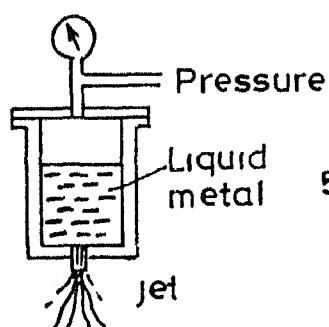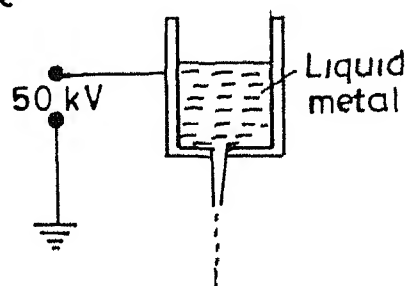
Fig 1 Schematical representation of major atomising processes

Growth of waves on sheet

Fragment-ation and formation of ligame-nts

Breakdown of ligments into drops
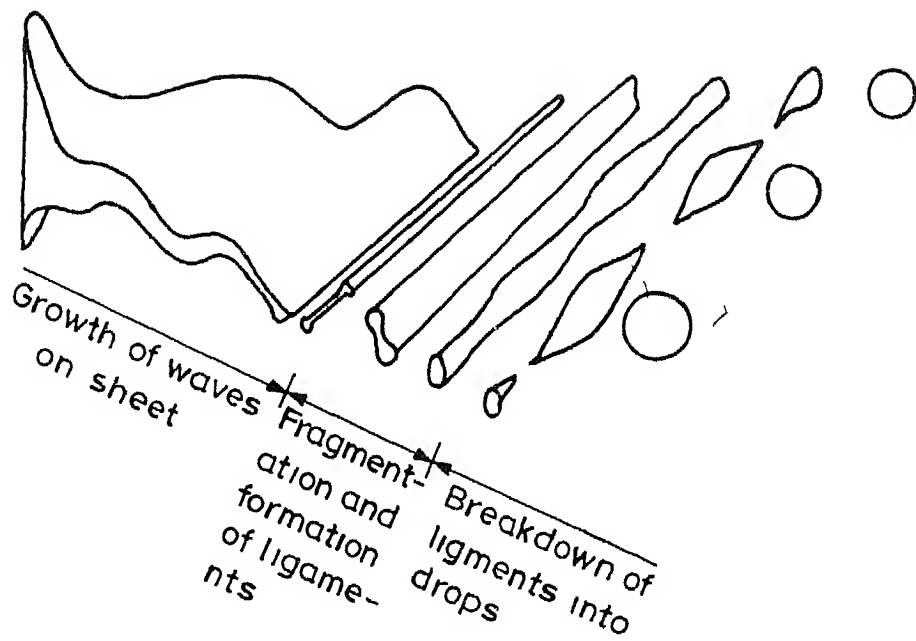
Fig 2 Formation of spherical droplets of liquid metal

Stage 1
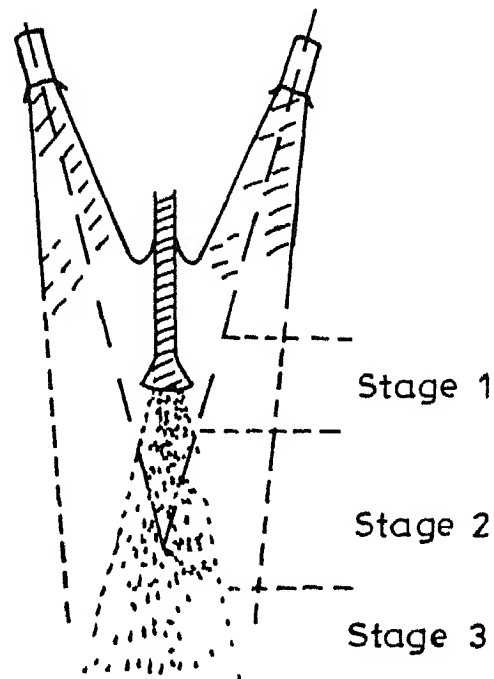
Stage 2

Stage 3

Fig 3 Different stages in gas atomisation of liquid metals
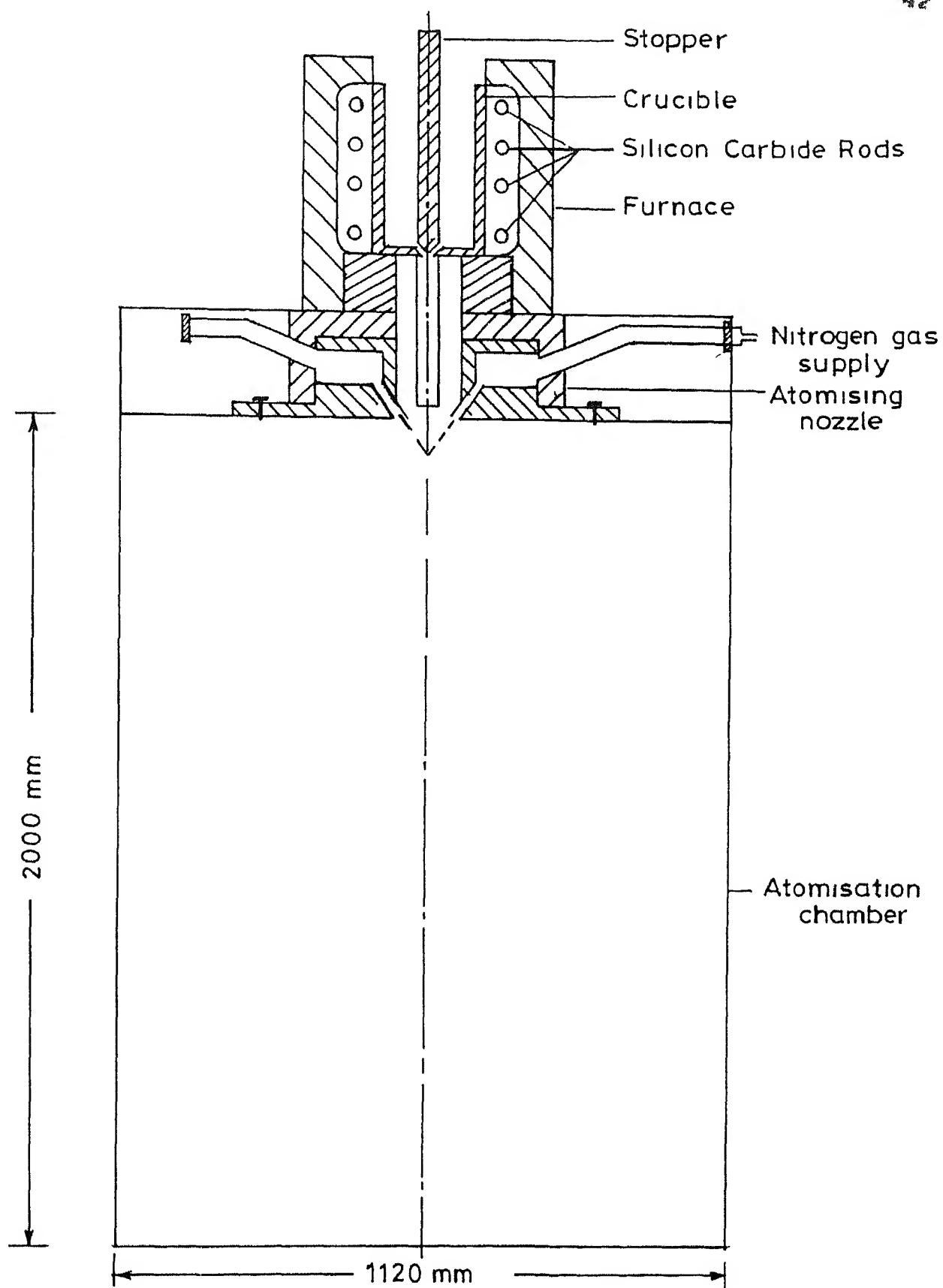
Fig 4 Schematic diagram of the experimental set up
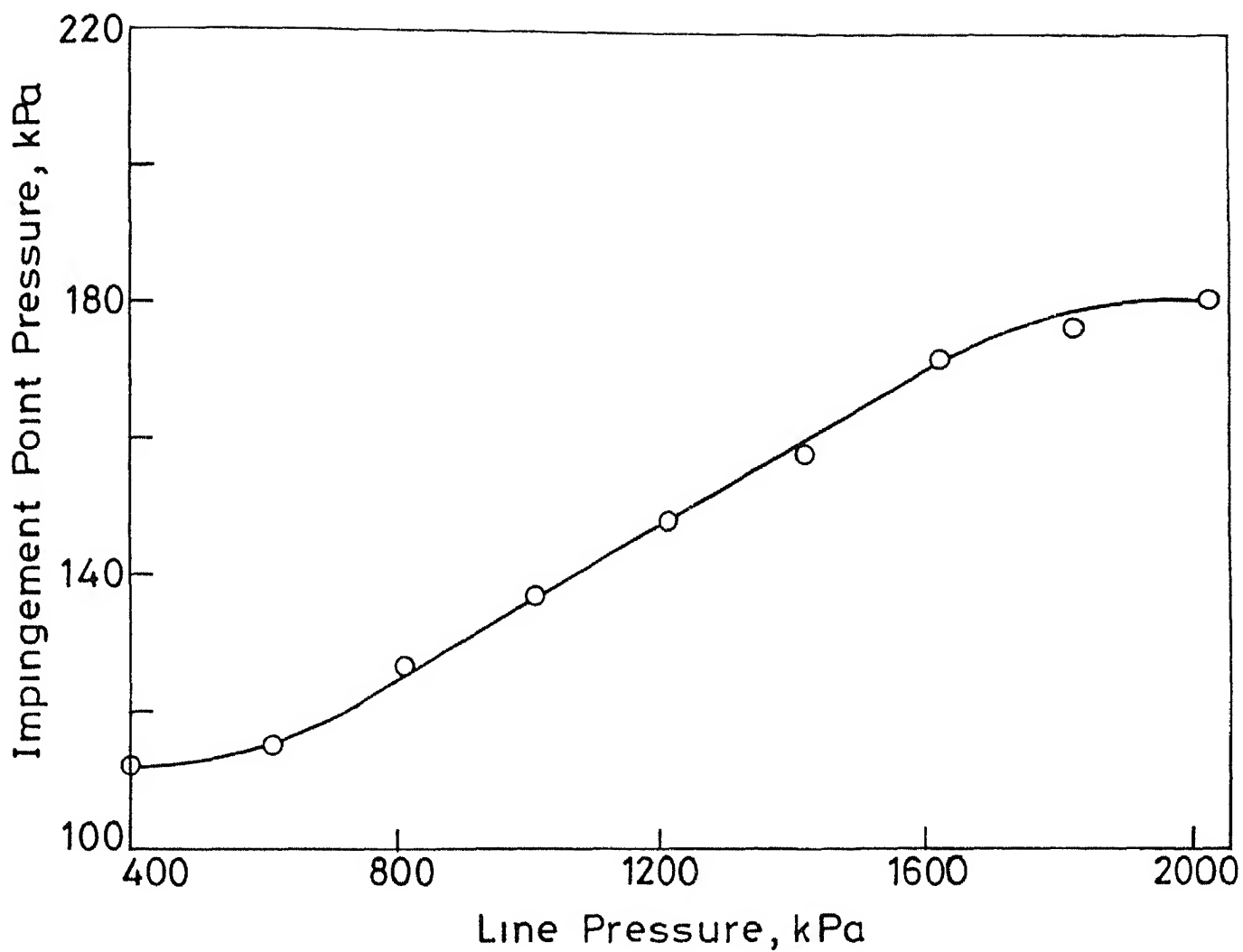
Fig 5 Relationship between impingement point pressure and line pressure
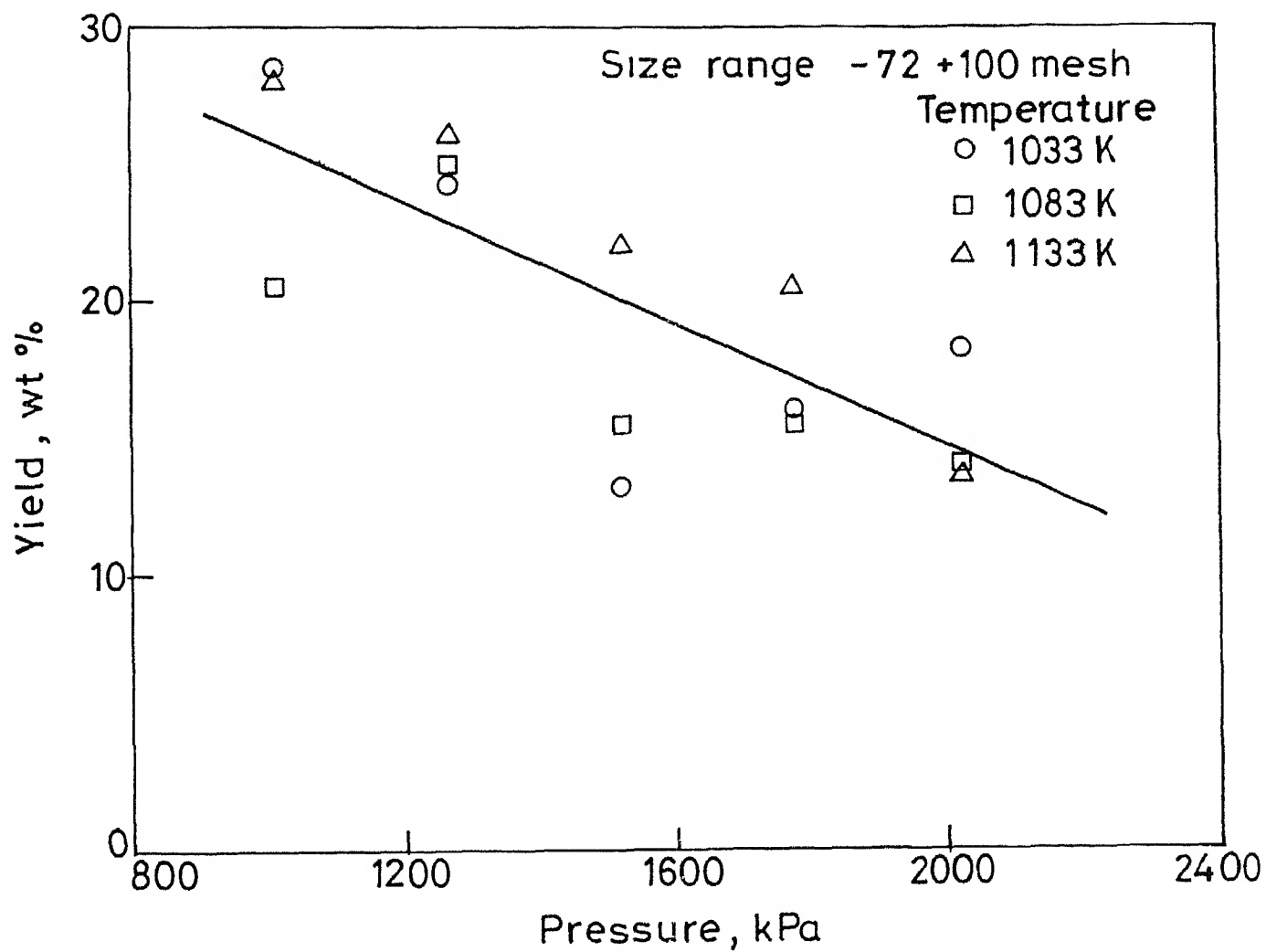
Fig 6(a) Yield as a function of line pressure in the
size range −72 +100 mesh
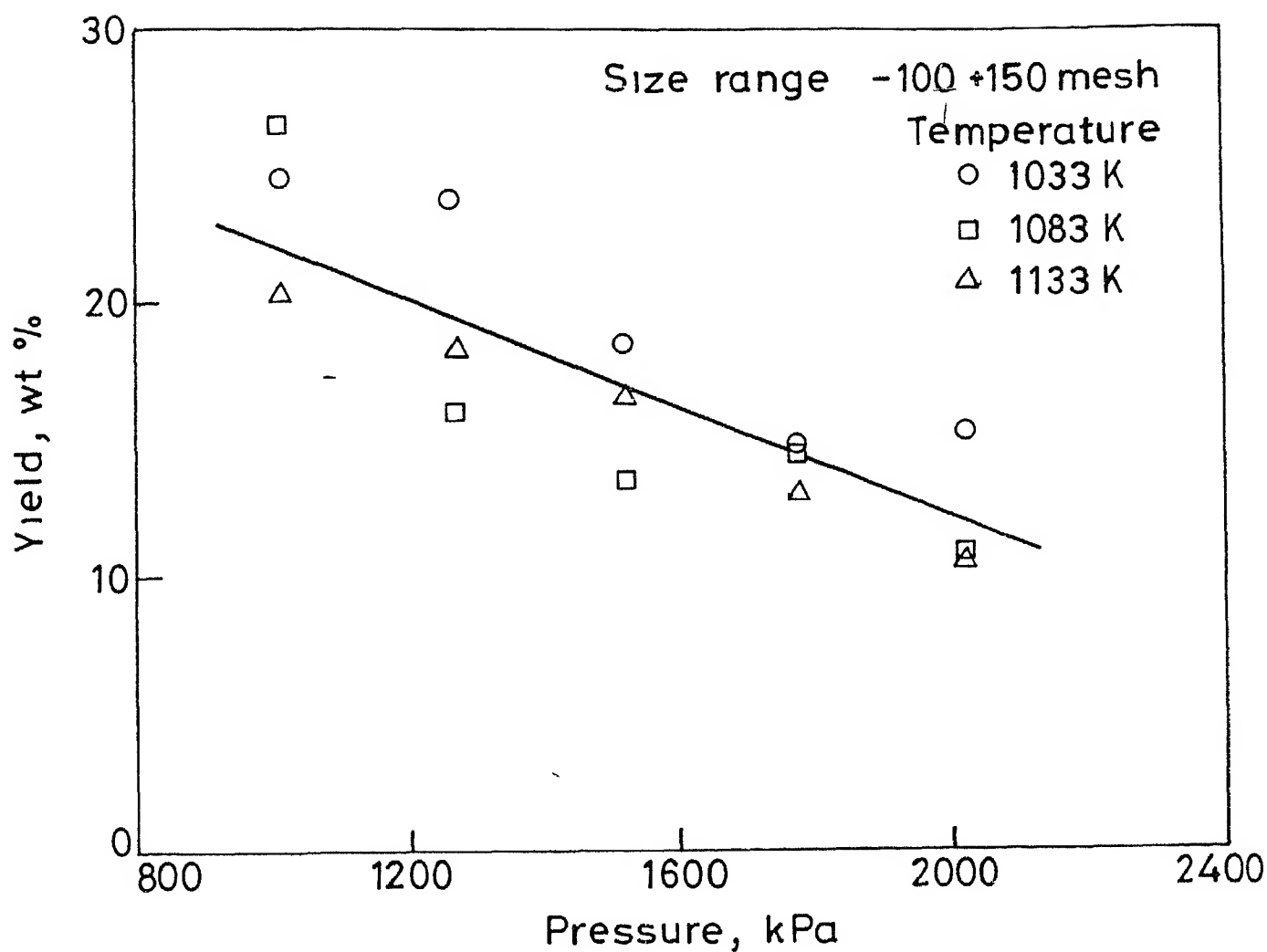
Fig 6(b) Yield as a function of line pressure in the size range −100 +150 mesh
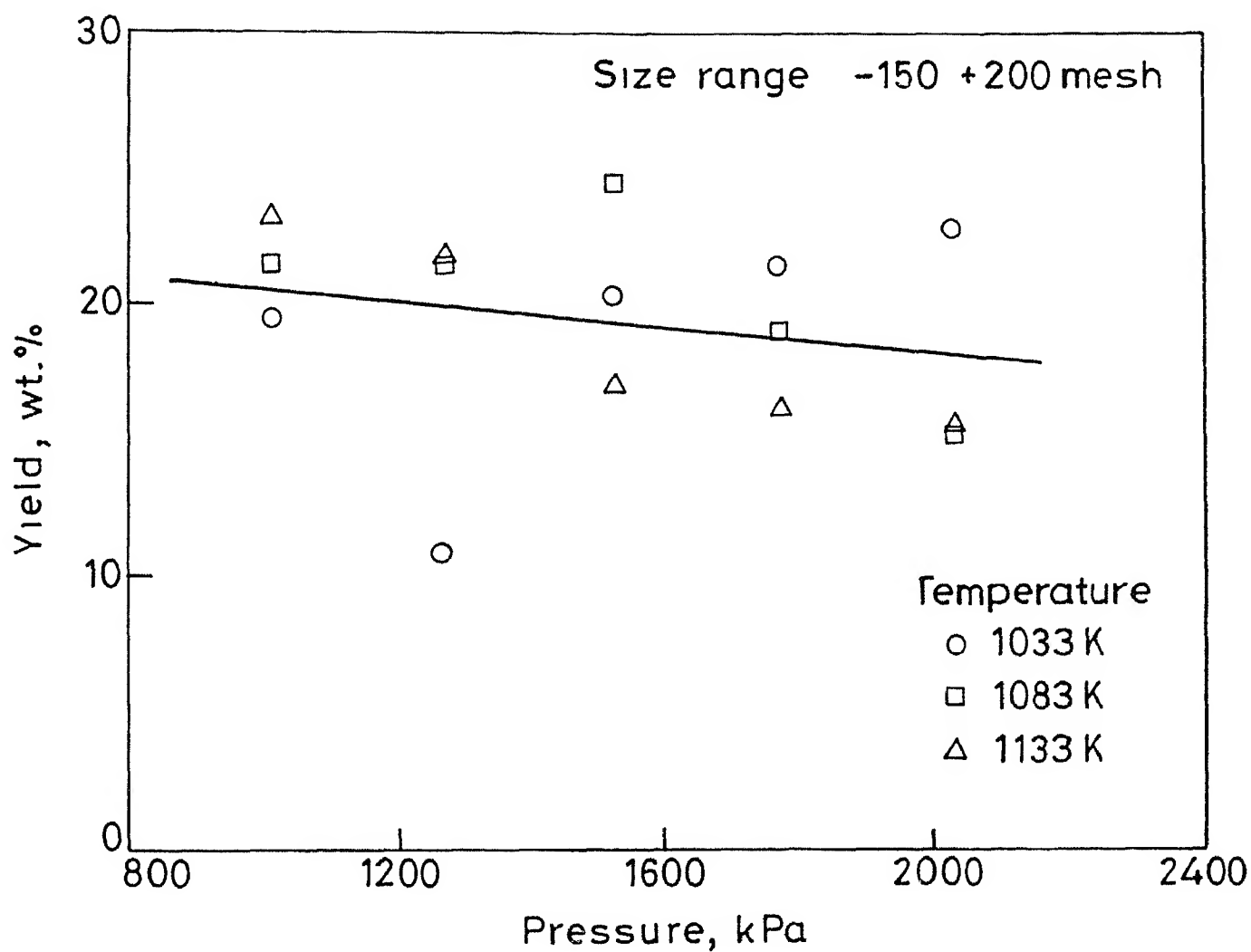
Fig 6(c) Yield as a function of the line pressure in the size range −150 +200 mesh
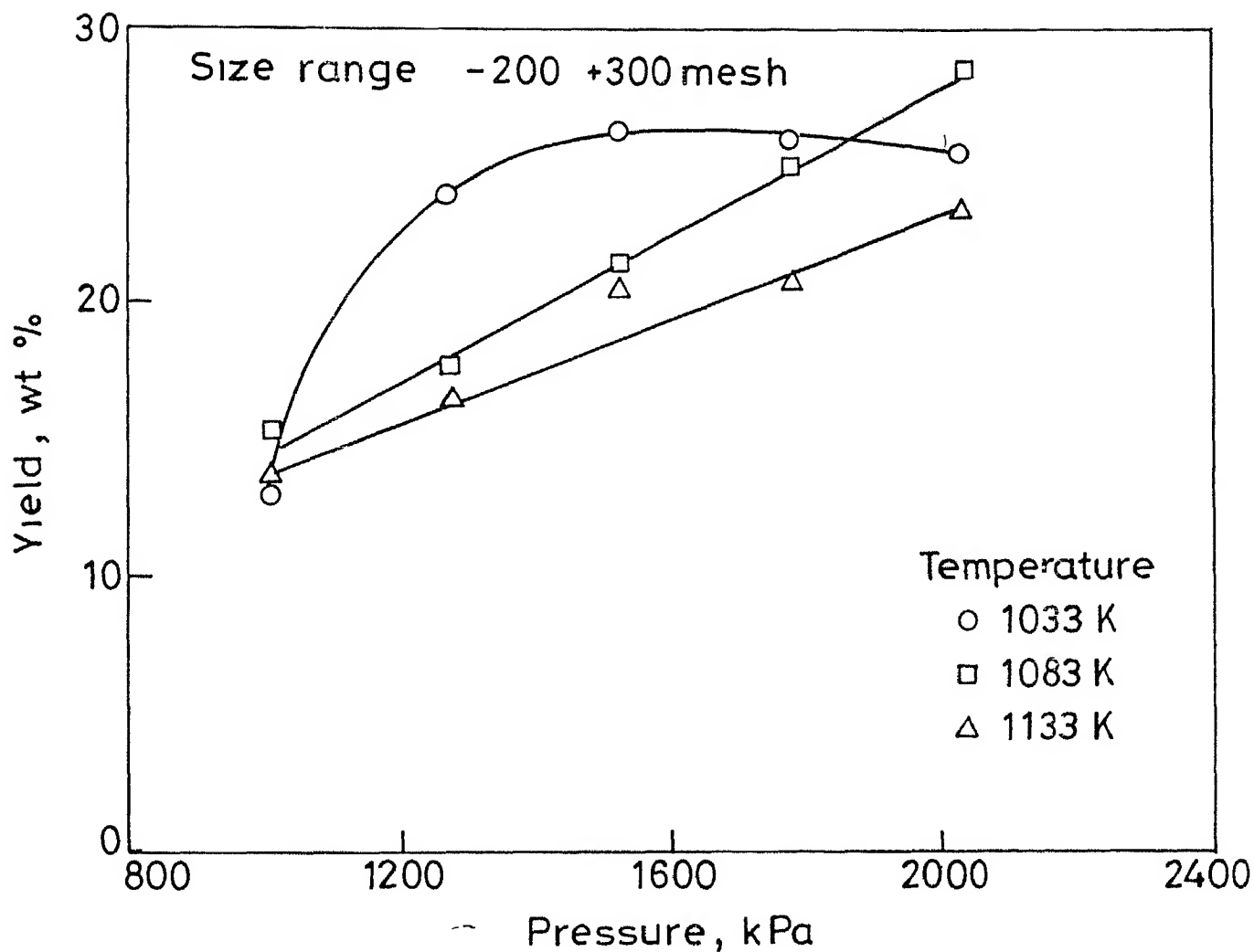
Fig 6(d) Yield as a function of line pressure in the size range −200 +300 mesh
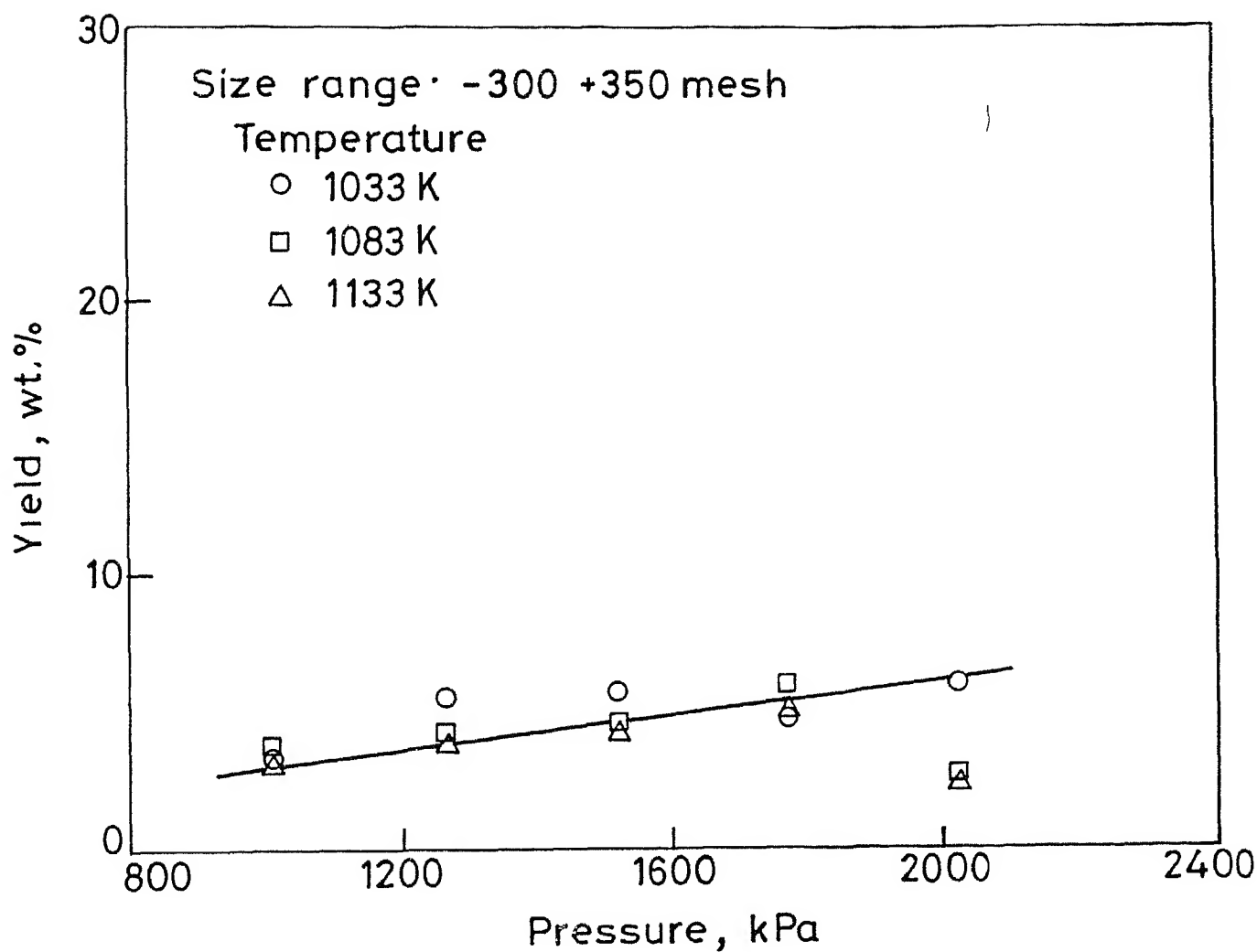
Fig 6(e) Yield as a function of line pressure in the size range −300 +350 mesh.
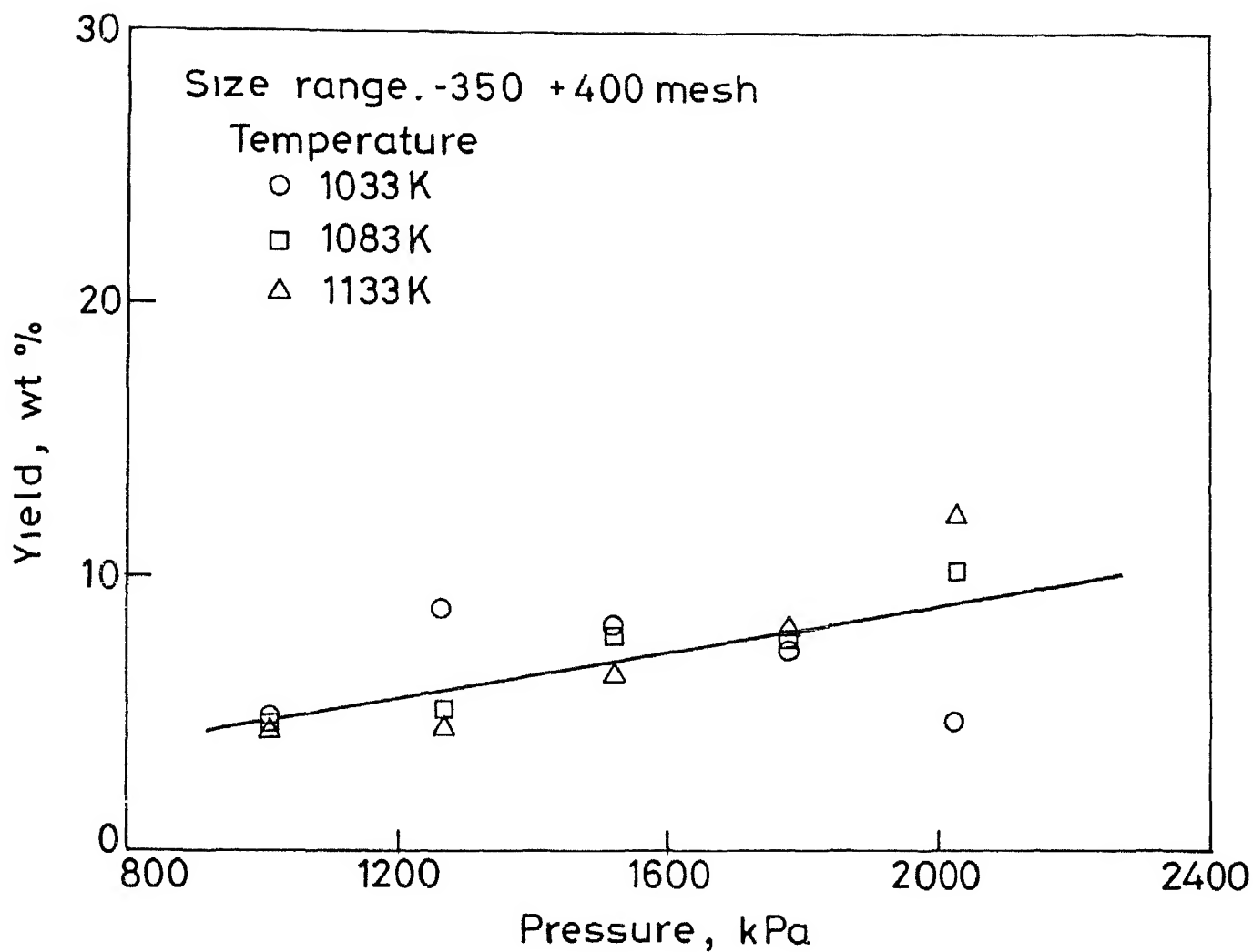
Fig 6(f) Yield as a function of line pressure in the size range -350 +400 mesh
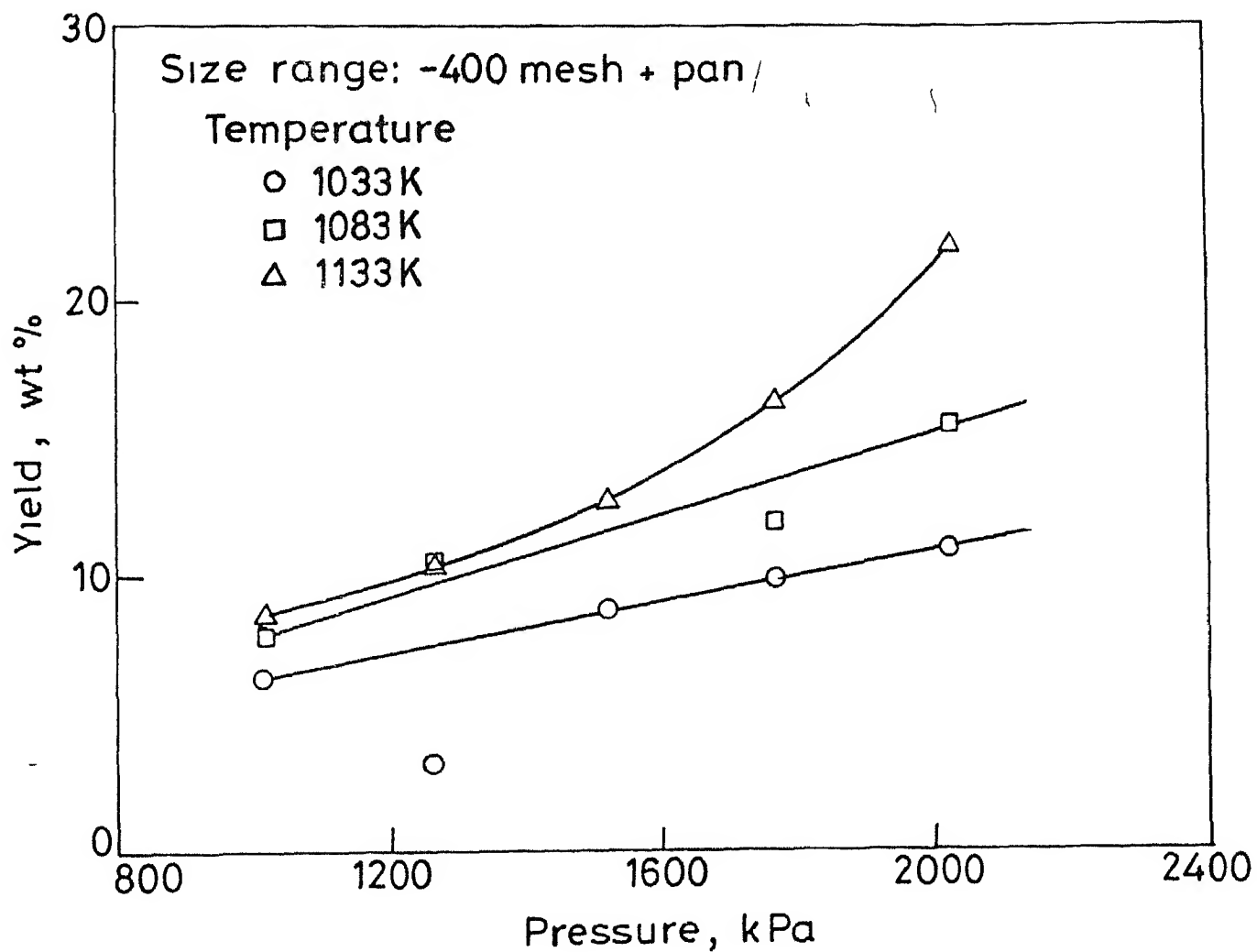
Fig 6(g) Yield as a function of line pressure in the size range -400 mesh + pan

Size range.

○	$- 72 + 100$
□	$-100 + 150$
△	$-150 + 200$
●	$-200 + 300$
■	$-300 + 350$
▷	$-350 + 400$
◀	$-400 + PAN$

Yield, wt%

Nitrogen Pressure at the Impingement Point, kPa
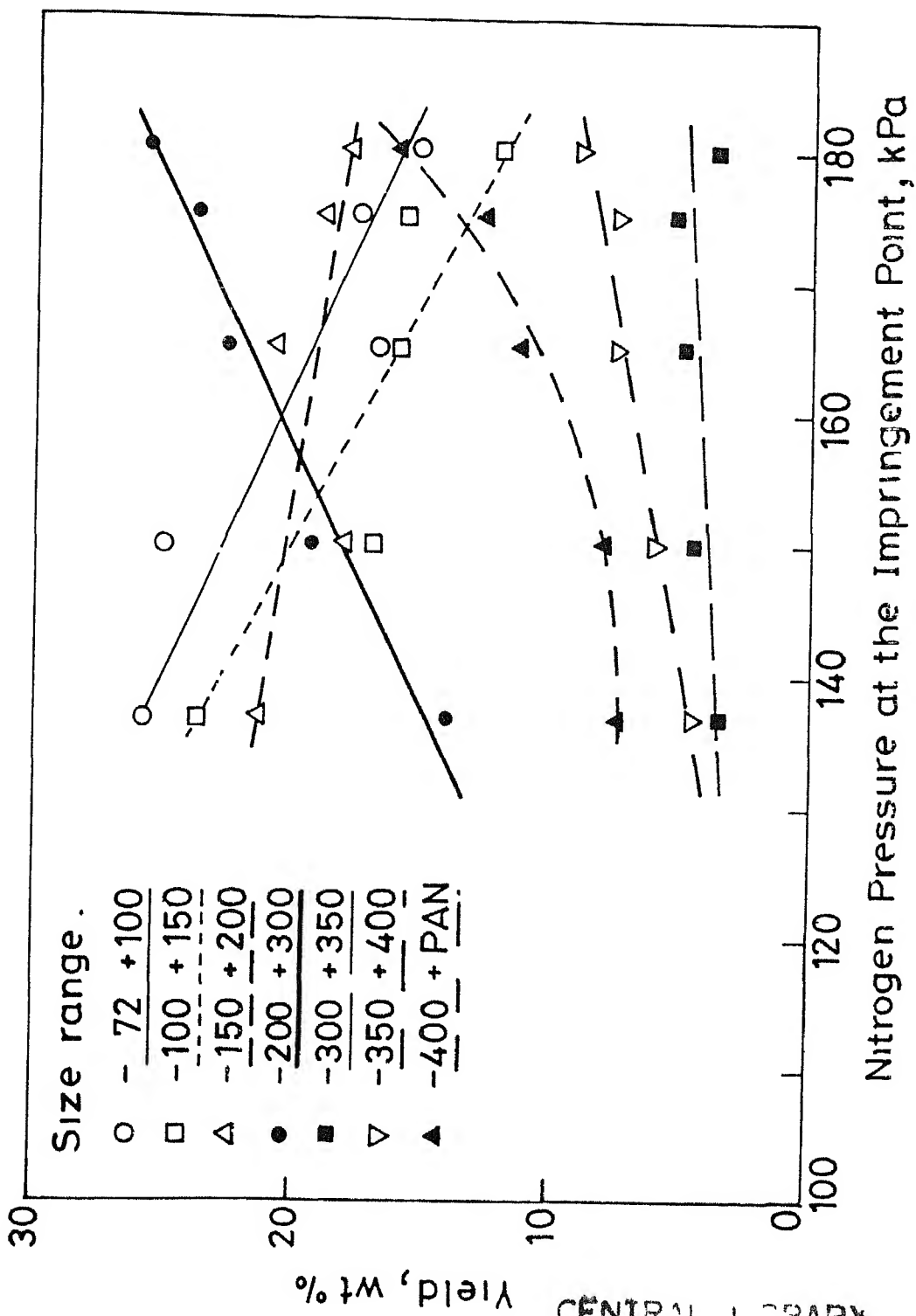
Fig 7 Yield in different size ranges as a function of impinge-
ment point pressure
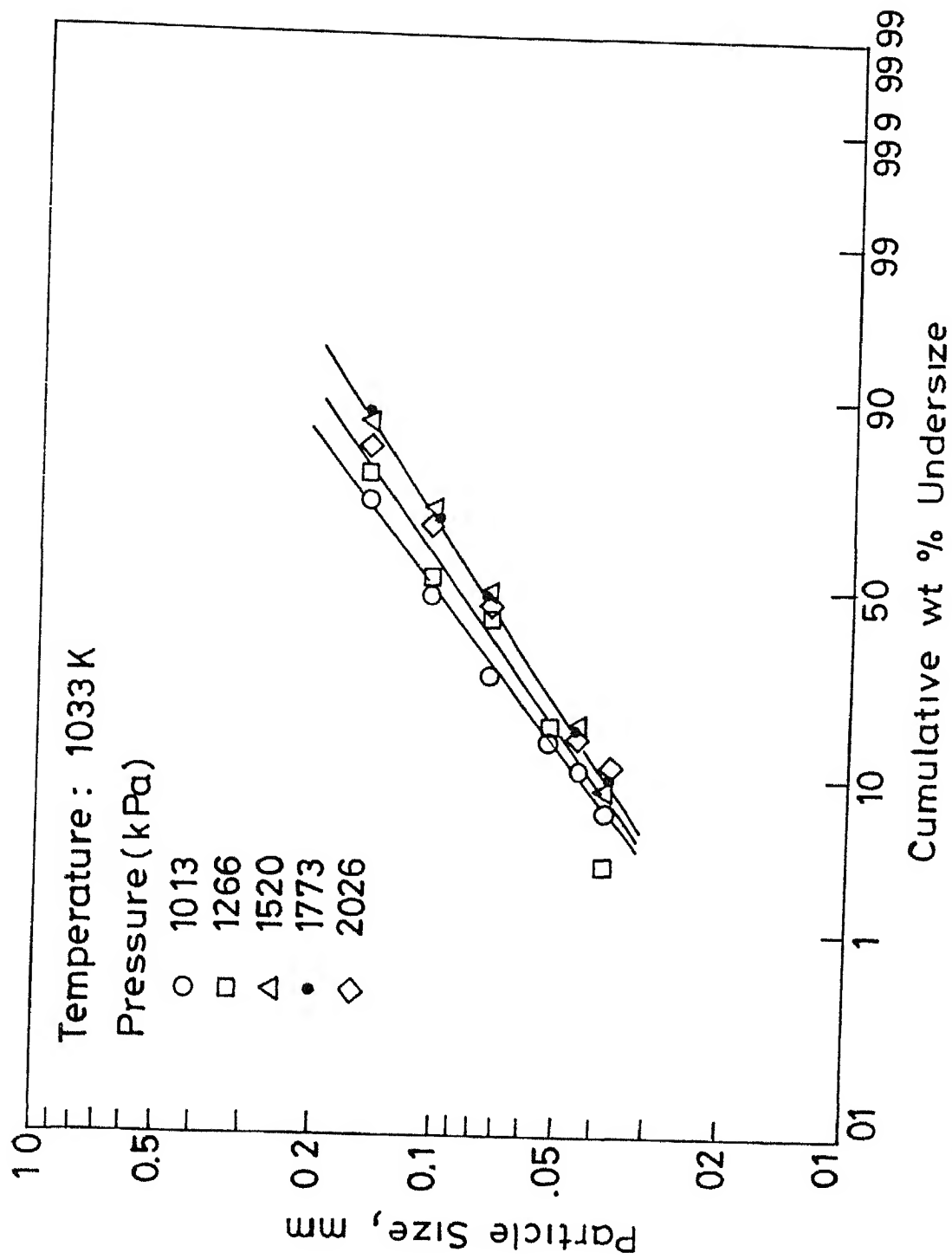
Fig 8(a) Plot between partical size and cumulative wt % undersize at 1033 K.
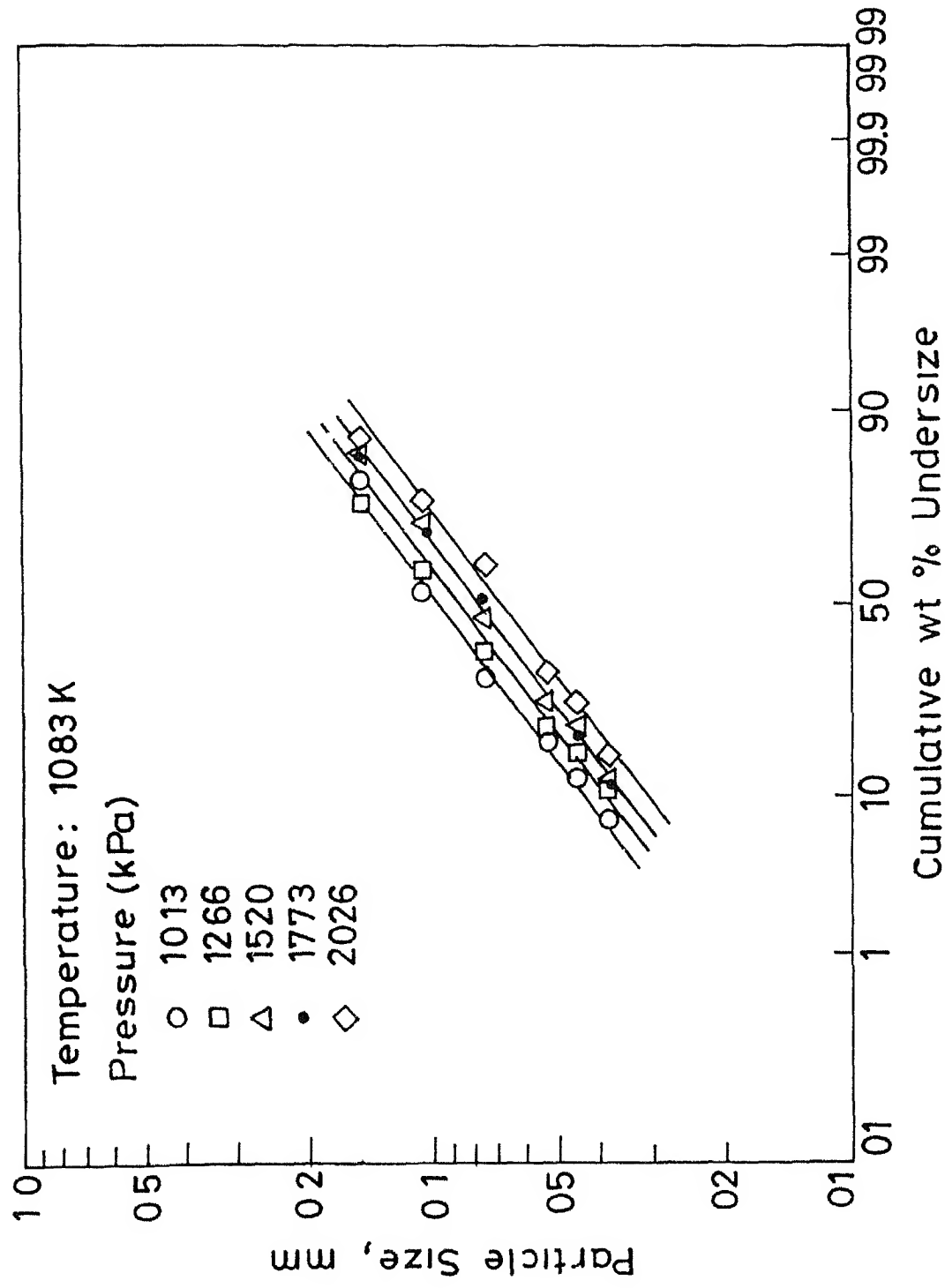
Fig 8(b) Plot between partical size and cumulative wt.% undersize at 1083 K
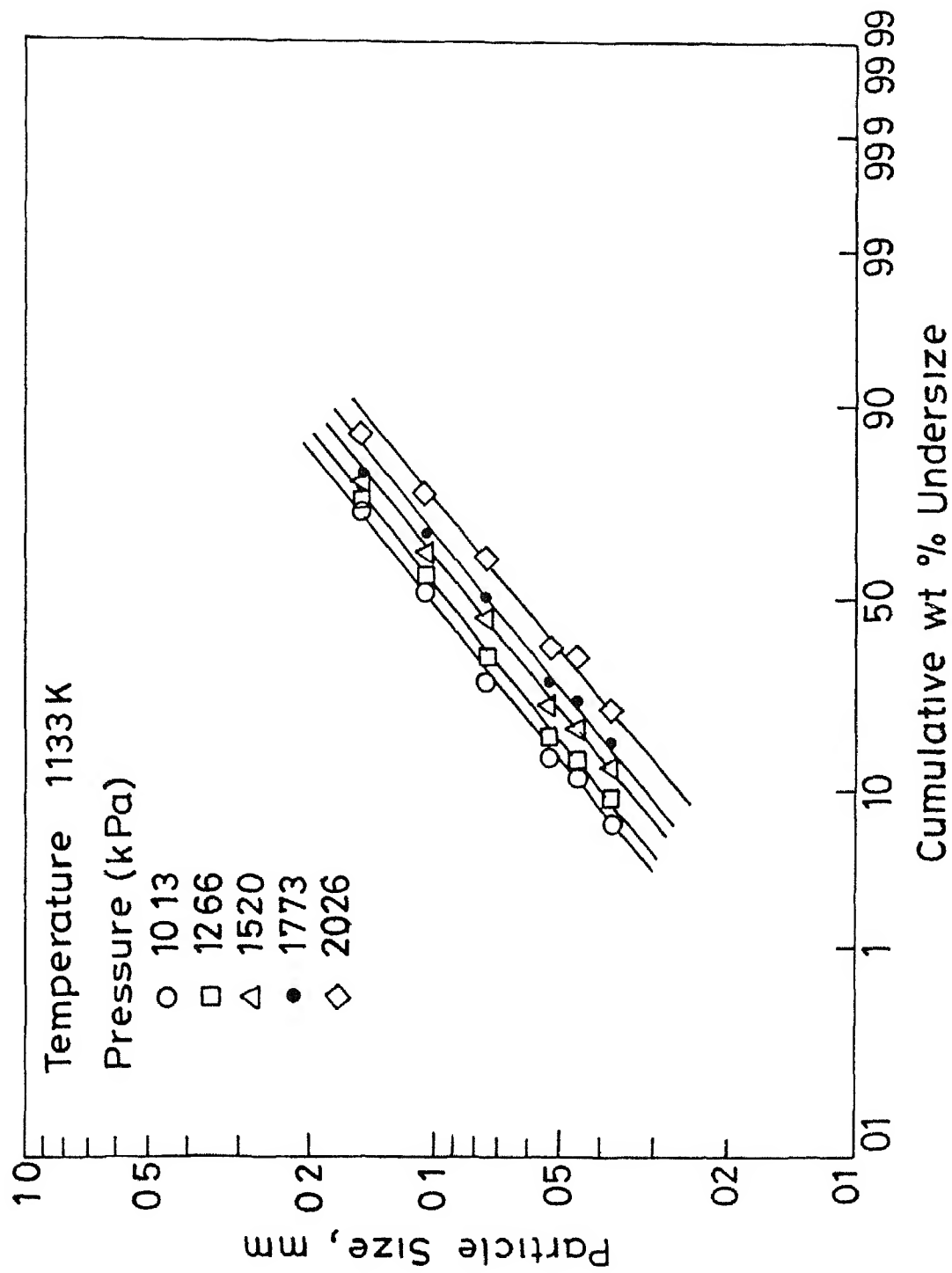
Fig 8(c) Plot between particle size and cumulative wt.%
undersize at 1133 K
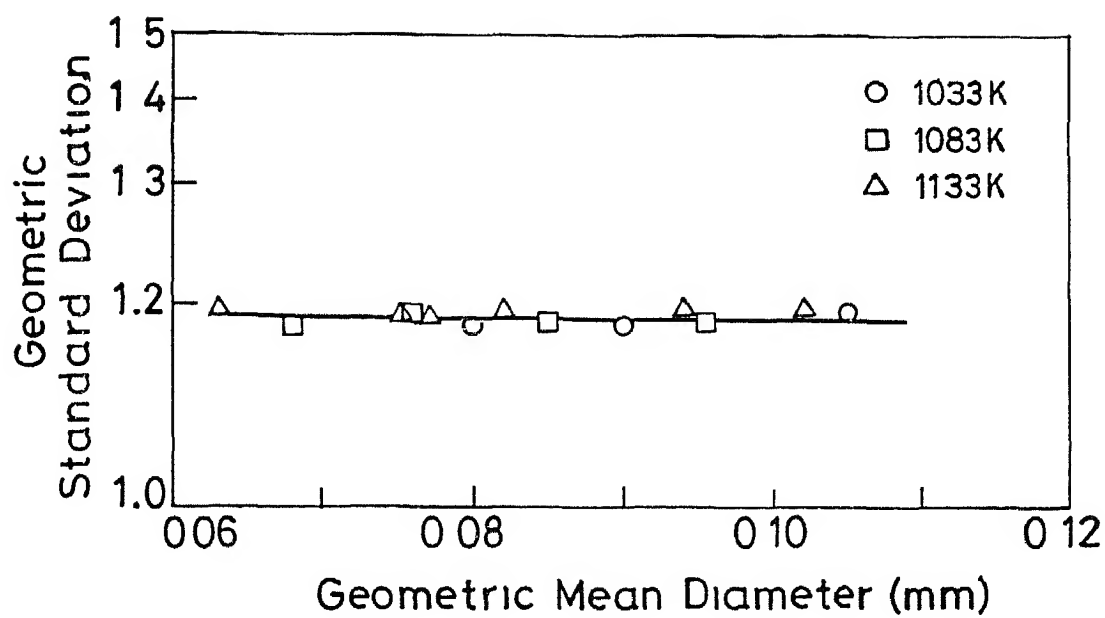
Fig 9 Relationship between geometric standard
deviation and geometric mean diameter
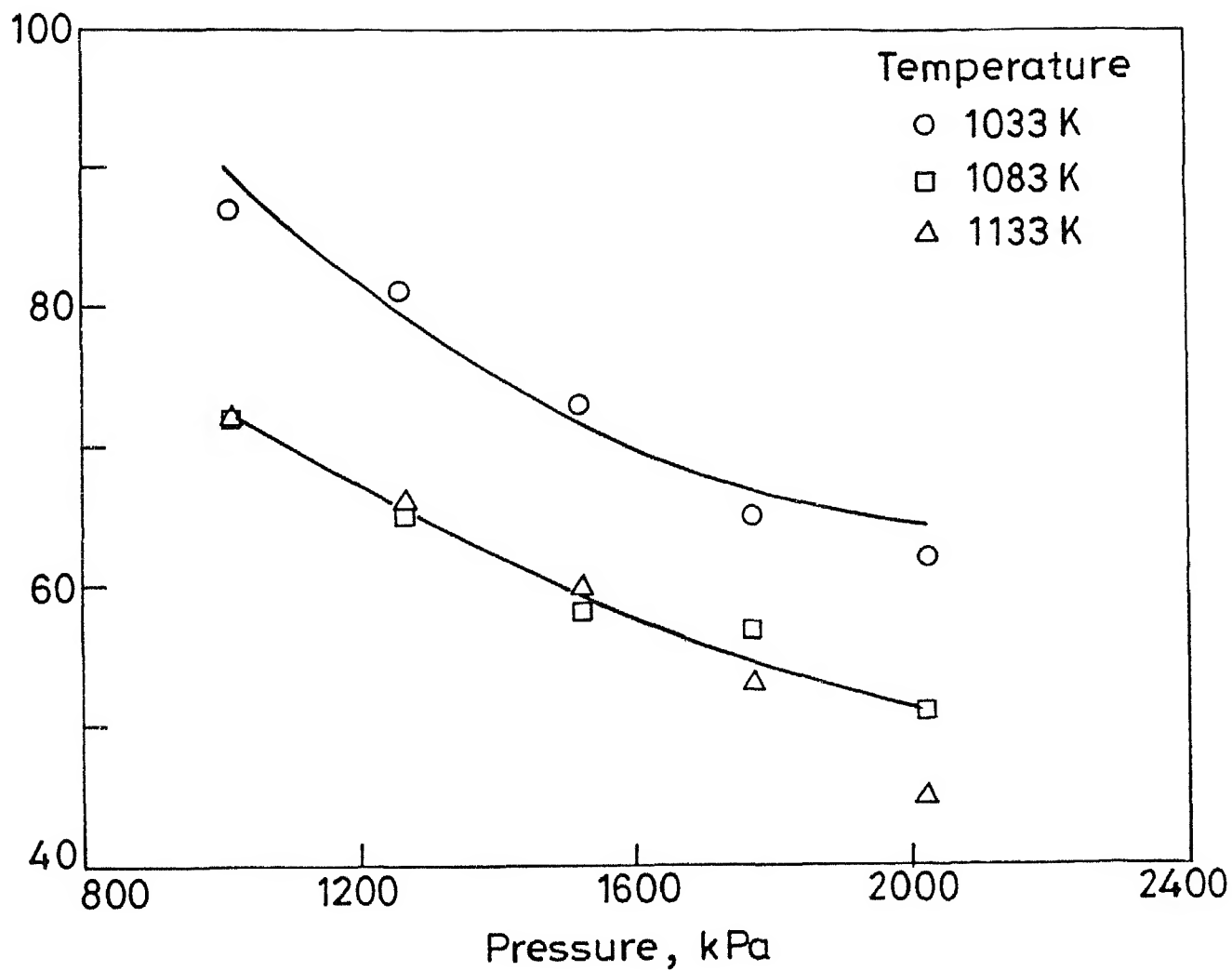
Fig 10 Effect of line pressure on Sauter mean diameter
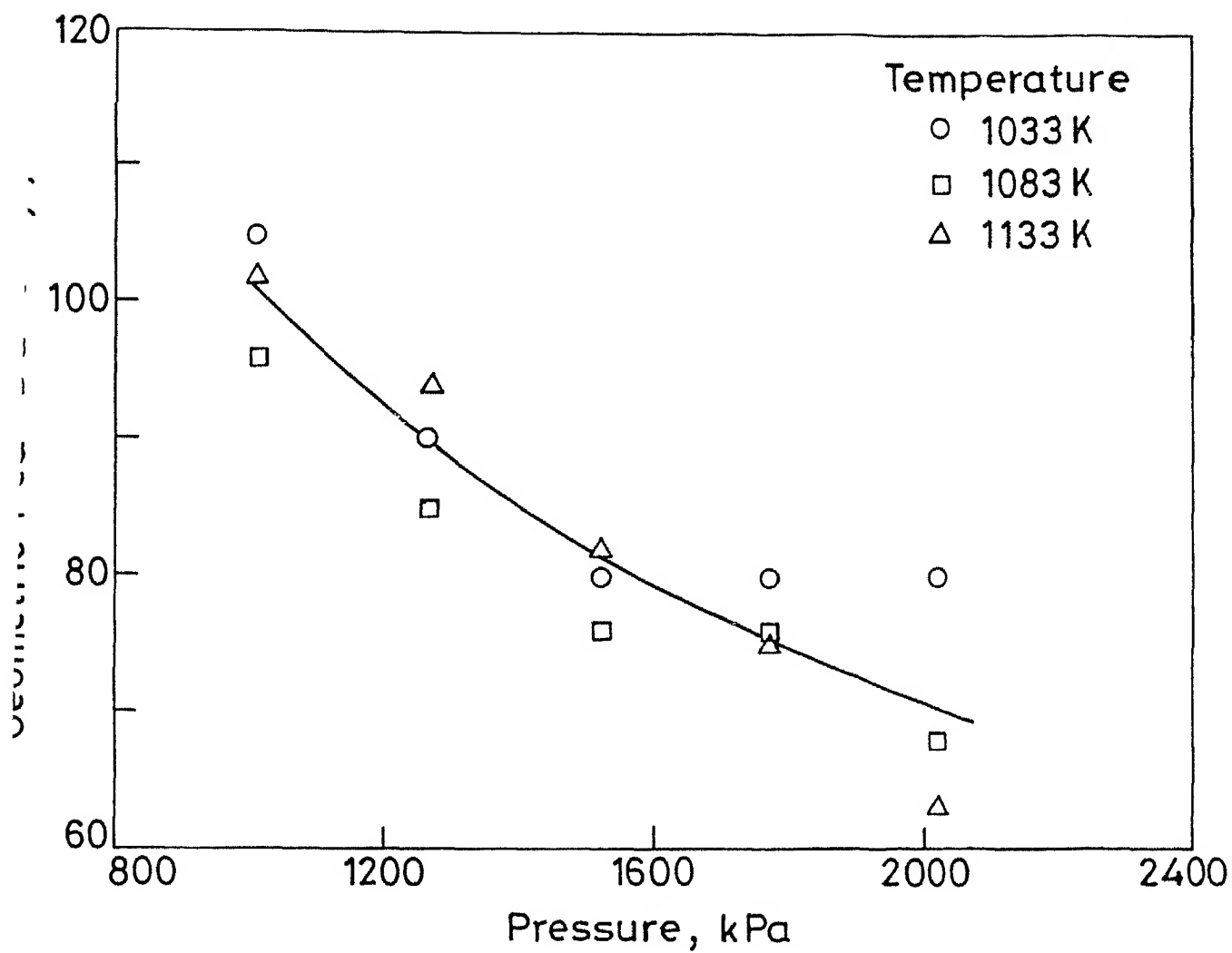
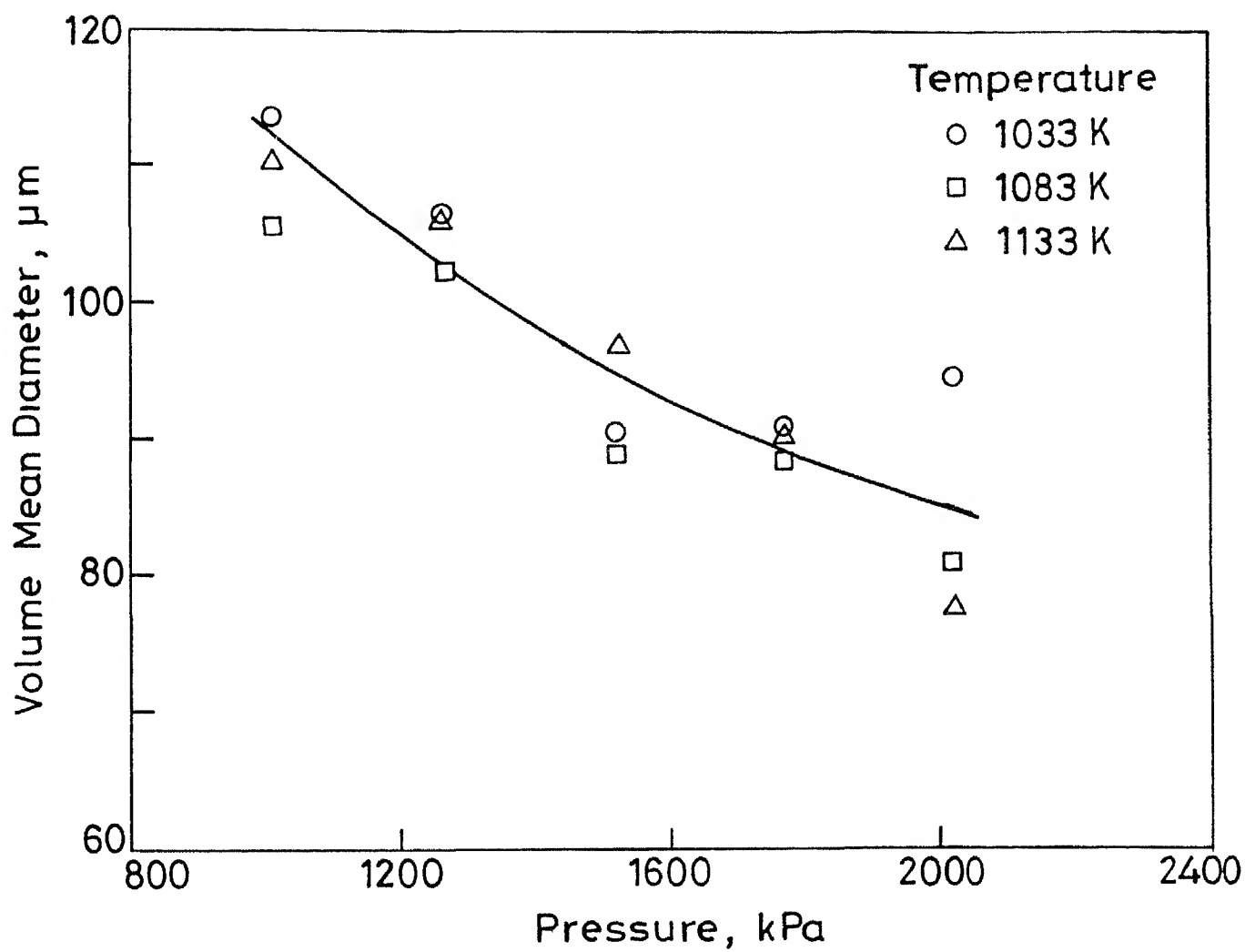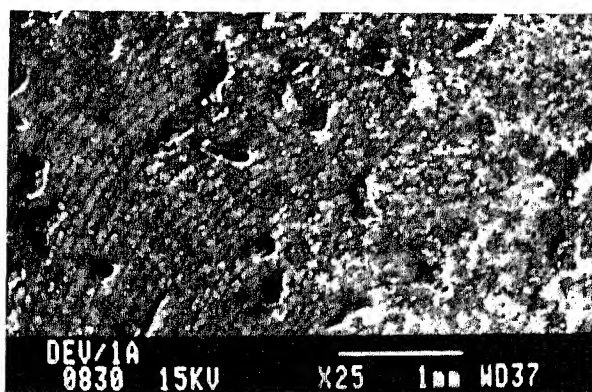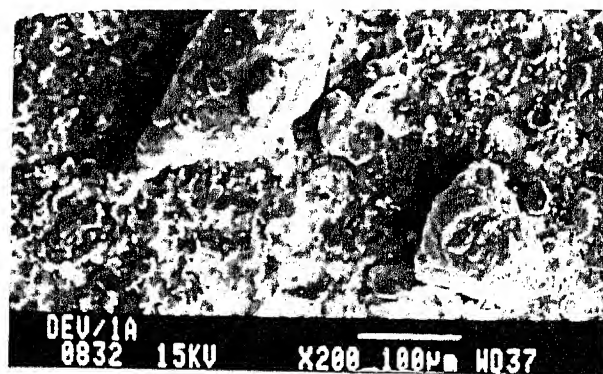Fig 11 Effect of line pressure on geometric mean diameter.

Fig 12 Effect of line pressure on volume mean diameter

(i)   (ii)

Fig. 13(a)   Scanning Electron Micrographs of aluminium
              powder in the size range : -100 + 150 mesh
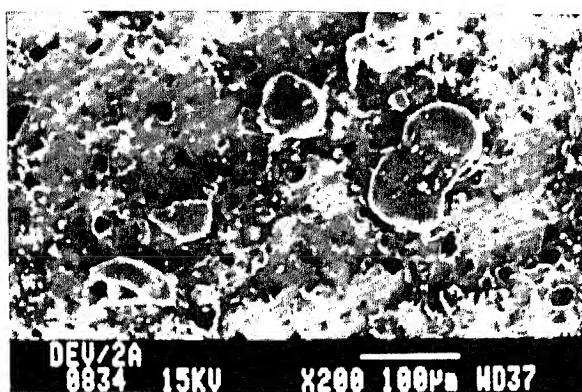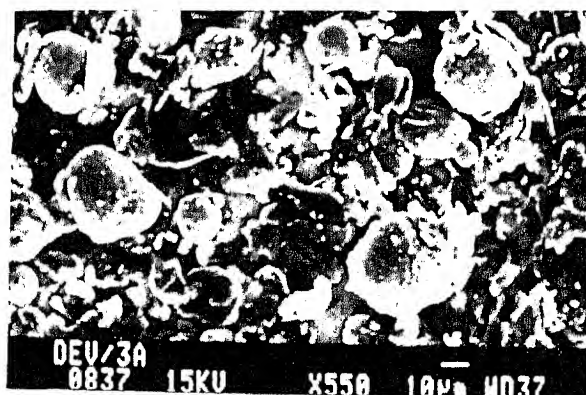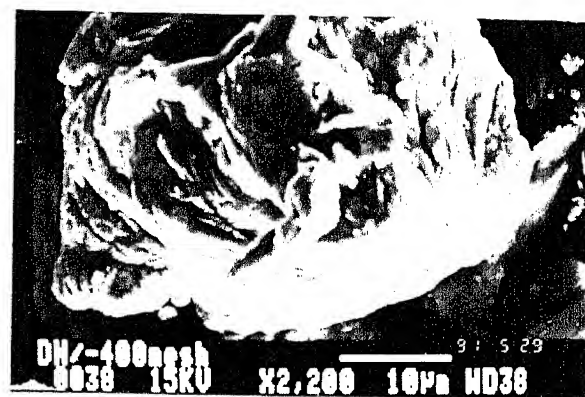
Fig. 13(b) Scanning Electron Micrograph of aluminium
powder in the size range : -200 + 300 mesh

(i)

(ii)

(iii)

Fig. 13(c)   Scanning Electron Micrographs of aluminium
             powder in the size range : -400 + PAN

REFERECNCES

1   Mehrotra, S P   Mathematical Modelling of Gas Atomisation Process for Metal Powder Production Part 1   Powder Metallurgy International 13 (1981) 80

2   See, J B , and Johnston, G H , Powder Technology, 21 (1978) 119

3   Dunkleg J J Atomization   A Brief Review Powder Metallurgy 29 (1986) No 1 10-12

4   Dube R K Koria, S C , Subramarian, R, Atomisation of Aluminium by Multiple Type Discrete Nitrogen Jets Powder Metallurgy International Vol 20 NO 6 (1988)

5   Unal, A , Production of Rapidly solidified Aluminium Alloy Powder by Gas Atomisation and their Application, Powder Metallurgy Vol 33, No 1 (1990) 53

6   Metals Hand book Volume 7 9th Edition, American Society of Metals

7   Lubanska H , Correlation of Spray Ring Data for Gas Atomisation of Liquid Metals Journal of Metals Feb (1970) 45

8   Unal, A , Effect of Processing variables on Particle size in Gas Atomisation of Rapidly Solidified Aluminium Powders Materials Science and Technology, Vol 3, Dec (1987) 1029

9   Thompson J S A Study of Process variables in the Production of Aluminium Powder by Atomisation, Journal of Institution of Metals, Vol 74, (1948) 101-132

10 Goulden C H , Methods of Satistical Analysis, 2nd Ed   Asia Publishing House (1959)

11 Design Data Handbood, PSC Publication (9187)

APPENDIX - 1

CALCULATION OF F-VALUES

Size Range   100 +150 mesh

Pressure (kPa)	Temperature , K 1033	1083	1133	Σy_1	Σy_1^2
1013	24 4	26 6	20 3	71 3	1715 01
1266	16 3	15 7	18 7	50 7	861 87
1520	18 0	13 5	16 6	48 1	781 81
1773	19 7	14 6	13 1	47 4	772 86
2026	15 2	10 6	10 5	36 3	453 65
Σy_j	93 6	81 0	79 2		

$\Sigma\Sigma \ y_{1j} \ = 253 \ 8$ y is yield in wt%

$\Sigma\Sigma \ y_{1j}^2 \ = 4585 \ 2$

correction factor $CF = \dfrac{(\Sigma\Sigma \ y_{1j})^2}{N}$

where N is total degree of freedom and is 15

$$CF = \frac{253 \ 8^2}{15} = 4294 \ 3$$

Total sum of squares, $TSS = \Sigma\Sigma \ y_{1j}^2 - CF$

$$= 4585 \ 2 - 4294 \ 3$$

$$= 290 \ 9$$

Temperature sum of squares, TempSS $\sum\limits_{1=1}^{3} \dfrac{Y_1^2}{5} - CF$

$$= \dfrac{93\ 6^2 + 81\ 0^2 + 79\ 2^2}{5} - CF$$

$$= 24\ 62$$

Pressure sum of squares, PrSS $= \sum\limits_{1=1}^{5} \dfrac{Y_1^2}{3} - CF$

$$= 216\ 45$$

Error sum of squares ErSS = TSS - TempSS - PrSS

$$= 49\ 83$$

Mean Temperature sum of squares,

$$M\ TempSS = \dfrac{TempSS}{Temp\ d\ o\ f}$$

Mean Pressure sum of squares

$$M\ PrSS = \dfrac{PrSS}{Pr\ d\ o\ f}$$

Temperature degree of freedom   = 2

Error degree of freedom   = 4

$$M\ TempSS = \dfrac{24\ 62}{2} = 12\ 31$$

$$M\ PrSS = \dfrac{216\ 45}{4} = 54\ 11$$

Mean Error sum of squares

$$MErSS = \dfrac{ErSS}{Er\ d\ o\ f}$$

$$= \dfrac{49\ 83}{8} = 6\ 23$$

Calculated F - value for temperature

$$F^T_{calc} = \frac{MTempSS}{MErSS} = \frac{12\ 31}{6\ 23} = 1\ 98$$

Calculated F-value for pressure

$$F^T_{calc} = \frac{MPrSS}{MErSS} = \frac{54\ 31}{6\ 23} = 8\ 69$$

APPENDIX - 2

CALCULATION OF SOLIDIFICATION TIME AND SPHERODISATION TIME.

Solidifacation time

$$\tau_s = \frac{dP}{6h_c} \left[C_p \, \ln \left(\frac{T_1 - T_g}{T_m - T_g} \right) + \frac{\Delta Hm}{T_m - T_g} \right]$$

where   d   =   particle diameter

p   =   density of aluminium

C_p =   heat capacity of aluminium

T_1 =   initial temp of metal

T_g =   gas temperature

T_m =   metlting point of alumium

h_c =   convective heat transfer coefficient

hc is given by

$$h_c = \frac{k}{d} [\, 2 + 0 \, 6* \, Re^{0 \, 5} \, Pr^{0 \, 33}]$$

where K is thermal conductivity of aluminium

Re is Reynold's number, $Re = \frac{\rho V_{re} d}{\mu}$

Pr is Prandle number, $Pr = \frac{\mu C_{p(gas)}}{k}$

V_{Rel} is relative velocity of gas and metal

μ is viscosity of liquid aluminum

$C_{p(gas)}$ is heat capacity of nitrogen gas

Relative Velocity V_{Rel}, is given by

$$V_{Rel} = \sqrt{\frac{KR}{Mg} * 0.833 \ T_g} \quad * \sqrt{\frac{K+1}{K-1} \left\{ 1 - (\frac{Pa}{Pb})^{\frac{K-1}{K}} \right\}}$$

where K is specific heat ratio

R is gas constant

Mg is molecular wt of N_2

Pa is atmospheric pressure

Pb is pressure of gas at the point of impengement

Spherodisation time

$$\tau_{sph} = \frac{3\pi^2 \ \mu l}{4 \ v \ \sigma} \ (r_1^4 - r_2^4)$$

where μl is viscocity of aluminium

σ is surface tension of aluminium

r_2 is particle radius

r_1 maximum radus ($\sim 10 r_2$)

v is volume of one particle

At 1520 kPa pressure and 9083 K temperature

$$V_{rel} = 288 \ m/sec$$

for particle of size 0.150 mm

$$Re = 2765.38$$

$$Pr = 0.7088$$

$$h_c = 5267$$

$$\tau_{sol} = 8.73 * 10^{-3} \ sec$$

& $\quad \tau_{sph} = 1.43 * 10^{-3} \ sec$

Ratio τ_{sol}/τ_{sph} = 6

For particle of size 0 038 mm

Re = 700 5

Pr = 0 7088

h_c = 1 12 * 10^4

τ_{sol} = 6 3 * 10^{-3}

& τ_{sph} = 3 63 * 10^{-4} sec

Ratio τ_{sol}/τ_{sph} ≃ 18